Heliyon 10 (2024) e32440

Contents lists available at ScienceDirect

Heliyon

journal homepage: www.cell.com/heliyon

Research article

The spinning disc reactor for photocatalytic degradation: A systematic review

Saeid Fallahizadeh [a,b], Mitra Gholami [a,b,*], Mahmood Reza Rahimi [c,**], Hamid Reza Rajabi [d], Shirin Djalalinia [e], Ali Esrafili [a,b], Mahdi Farzadkia [a,b], Majid Kermani [a,b]

[a] Research Center for Environmental Health Technology, Iran University of Medical Sciences, Tehran, Iran
[b] Department of Environmental Health Engineering, School of Public Health, Iran University of Medical Sciences, Tehran, Iran
[c] Process Intensification Laboratory, Department of Chemical Engineering, Yasouj University, Yasouj, 75918-74831, Iran
[d] Chemistry Department, Yasouj University, Yasouj, 75918-74831, Iran
[e] Deputy of Research & Technology, Ministry of Health & Medical Education, Tehran, Iran

ARTICLE INFO

Keywords:
Spinning disc reactor
Photocatalytic degradation
Pollutants
Reaction kinetics

ABSTRACT

In recent years, the use of a horizontal spinning disc reactor (SDR) as a photocatalytic reactor for the degradation of various pollutants in aqueous solutions has increased. This study was searched based on the PRISMA method. Two autonomous researchers carried out for the relevant studies using Scopus, Web of Science (WOS), and Science Direct databases. The search terms expanded focusing on the performance of horizontal spinning disc photocatalytic reactor (SDPR). In this review article, the main objective of the effect of operational factors on the efficiency of the degradation of pollutants with changes in the type of light source (range of visible light and UV radiation), disc rotational speed, flow rate, initial concentration of pollutants, pH, type of disc structure and flow regime are considered. Current challenges in SDPR include issues such as limited mass transfer, uneven light distribution, and difficulties in scaling up. To overcome these challenges, improvements can be made by optimizing reactor design for better mass transfer, enhancing light distribution through advanced light sources or reactor configurations, and developing scalable models that maintain efficiency at larger scales. Additionally, the use of innovative materials and coatings could improve the overall performance of SDPR.

1. Introduction

Discharge of industrial, agricultural, and other human activities releases various types of chemicals into the water and natural environments and pollutes existing water resources [1,2]. Hazardous chemicals such as pesticides, dyes, chlorinated pollutants, heavy metals, drugs, Antibiotics, endocrine disrupting chemicals (EDCs), personal care products, pharmaceutical products (PPCPs), and their conversion products enter water environments through these types of wastewater [3–6]. The pollution of water resources is a problem that due to the entry of a wide variety of pollutants is becoming acute today [7]. Chemical pollution due to solvents, dyes, heavy metals, etc., is considered a great threat to water quality [8,9]. This pollution is caused by the tremendous use of organic and inorganic

* Corresponding author. Research Center for Environmental Health Technology, Iran University of Medical Sciences, Tehran, Iran.
** Corresponding author. Process Intensification Laboratory, Department of Chemical Engineering, Yasouj University, Yasouj, 75918-74831, Iran.
E-mail addresses: gholamim@iums.ac.ir (M. Gholami), mrrahimi@yu.ac.ir (M.R. Rahimi).

https://doi.org/10.1016/j.heliyon.2024.e32440
Received 31 January 2024; Received in revised form 2 June 2024; Accepted 4 June 2024
Available online 4 June 2024

Table 1
Summarizes the different advantages and disadvantages of the suspended/slurry and immobilized/deposited photocatalytic reactors.

Reactor	Advantages	Disadvantages	Reference
Slurry/Suspension	❖ Massive total surface area ❖ Irradiated photocatalytic surface area to reactor volume has higher ratio. ❖ Adsorption of reactants onto the catalyst surface before entering reactor ❖ Particles in the form of suspension have better mixing. ❖ High mass transfer ❖ more effective active sites ❖ There are almost no mass transfer limitations. ❖ The effects of fouling by catalyst are largely minimized, if the catalyst in the reactor is continuously added and eliminated. ❖ Distribution of catalysts is uniform.	❖ Continuous mixing needed to prevent powders from precipitating ❖ To recovery of the photocatalyst from the treated effluent streams requires expensive secondary treatment filtration processes. ❖ The smaller the powder size, the more difficult it is to catalyst recovery ❖ At higher catalyst concentrations, suspended/slurry catalysts tend to cause light scattering, therewith reducing the rate of photocatalytic reactions. ❖ shading effect decreases the penetration of photons deep into the pollutant solution ❖ Catalytic particles accumulate especially at higher concentrations.	[56–62]
Deposited/ immobilized	❖ It is very easy to separate the catalyst from the ultimately treated effluent stream. ❖ It can provide continuous reactor operation. ❖ Removal of organic matter from the liquid phase is improved by the use of immobilizing agents with adsorption properties.	❖ Catalyst deactivation and catalyst leaching are possible. ❖ Lower catalyst availability to photons. ❖ Significant limitations on external mass transfer at low pollutant flow rates ❖ Increasing the thickness of the catalyst film may cause internal mass transfer.	

pollutants from agricultural, urban, and industrial sources (such as the textile and pharmaceutical industries) [10,11]. Some of these origins of pollutants are not only sources of emerging pollutants (EPs), but also contribute to the release and re-entry of these pollutants into aquatic environments [7,12]. Synthetic drugs used in the pharmaceutical industry are one of the most dangerous pollutants. Also, pharmaceutical compounds, especially antibiotics used in medical and veterinary uses in the pharmaceutical industry are among the most dangerous emerging pollutants [13]. Due to industrial products, pollution is mainly caused by discharging waste into rivers and water bodies. To maintain and improve the quality of water around factories at a low cost for the profit of the people, many treatment techniques have been developed to treat polluted water. Therefore, the removal of pollutants from water bodies is very necessary for water quality conservation and improvement. Removing environmental pollutants using physical, chemical, and biological methods is often inefficient, expensive, and unsafe [14,15]. Physical methods (e.g. filtration and coagulation, reverse osmosis, adsorption), chemical methods (e.g. Ion exchange (IX), oxidation, advanced oxidation processes), and biological methods (e.g. biological degradation) have been used over the years in the treatment of municipal wastewater and industries [16–20]. However, most of these methods are time-consuming, expensive, and produce secondary contaminants [21]. Most of the common water and wastewater treatment procedures are not able to effectively remove resistant pollutants and as a result cannot meet the strict water quality standards, so alternative methods are needed [22,23].

As a result of these treatment methods, the advanced oxidation process (AOPs) as adsorption and degradation technique is attended an effective method for the complete mineralization of organic and inorganic effluents into eco-friendly products [20,24]. The advantages of applying AOPs for water and wastewater treatment include rapid degradation, reactions can happen at room temperature, complete mineralization of organic compounds, other residual oxidants, elimination of effects from disinfectants and degradation by-products of past treatments [25,26]. Also, the AOPs do not require external energy, they do not produce sludge, pollutants can be treated at low concentrations, and can be used for persistent pollutants to biodegradation before biological treatments [27,28].

A wide variety of reactor configurations have been reported in the literature. In general, photocatalytic reactors are divided based on the light source (UV and LED lamps), geometric shape (rectangular, square, cylindrical, and tubular), catalyst, liquid stirring method, bed dynamics (fixed bed and fluid bed) and the type of reactor. One of the types of classification of reactors is based on the type of catalyst selected for slurry and immobilized/deposited reactors [29]. In the deposited reactor, the catalyst can be coated on the substrate of the reactor, preserved on a solid substrate or coated using backing materials such as, silica, glass, alumina, zeolite and polymeric membranes [30–32]. The difference between the configurations of these two reactor categories is that slurry/suspension reactors need a secondary segregation unit to recover the photocatalyst in cases where the flow is applied continuously. In addition, at higher concentrations, the solution becomes duller and the penetration depth of light decreases, and due to the reduction of active photocatalytic sites, the degradation efficiency decreases [33,34]. To overcome these limitations, photocatalytic reactors are used that catalyze different substrates such as glass, quartz, alumina, ceramics, stainless steel, activated carbon and zeolite [10,35–38]. But this method leads to limitations in mass transfer. The contact surface decreases relative to the state where the particles are suspended in the reactor by deposition of the photocatalyst particles [39]. The relationship between efficiency, investment and operating costs determines the economic viability of a method. Therefore, the use of a photocatalytic method on an industrial scale is subject to the elimination of the limitations mentioned in this method. Therefore, a spinning disc reactor is one of the multipurpose devices which has been used so far to investigate biodiesel production, enzymatic reactions, nanoparticles synthesis, heat and mass transfer quick and homogenous mixing in a continuous operation, photocatalytic degradation of pollutants in aquatic environments and the effects of flow regimes on photocatalytic degradation and et cet [40–47]. Recently, this type of reactor (SDR) has been considered as a photocatalytic system for the degradation of textile and resistant pollutants such as pharmaceutical compounds and antibiotics [48–50]. To overcome the limitations mentioned above a spinning disc reactor is evaluated as a photocatalytic reactor [51]. A spinning disc reactor is a device in which mixing and mass transfer processes are intensified by creating a centrifugal field. Restriction of the photocatalytic degradation process that reduces efficiency is the lack of exposure of the photocatalyst to light. The farther away the catalyst is from the light source, because the intensity of the light is not sufficient to activate the catalyst surface, the catalyst activity decreases and therefore the degradation efficiency decreases. Therefore, designing a new system that can overcome this limitation seems necessary. A photocatalytic reactor based on a spinning disc in the process of photocatalytic degradation can also overcome the mentioned optical limitations. In the spinning disc system, owing to the centrifugal force of the liquid film, it forms fine droplets and thin layers. Light can easily reach the catalyst surface, increase the photocatalytic activity, produce more free radicals, and increase degradation efficiency.

In a slurry/suspension photocatalytic reactor, the recovery of catalyst particles from the obtained product is a time-consuming step, especially for catalyst particles with nanoscale properties (high surface area) [52]. To this end, photocatalytic reactors due to the use of deposited catalysts have been attracted a lot of attention [53,54]. This type of reactors can be used as a continuous system because there is no need to recover the catalyst. The significant blind spot of these immobilized catalysts backing reactors is that the degradation efficiency of target pollutants has been lower than the slurry/suspension reactors. This is due to the lack of systematic analysis of the interaction between fluid dynamics and reaction kinetics for these types of reactors and the low reaction rate, mainly due to the limited mass transfer of reactant species to photocatalytic surfaces. Therefore, according to the mentioned disadvantages of photocatalytic reactors based on the type of catalyst application, the SDR was experimented and evaluated for its efficiency as deposited catalyst photocatalytic reactor with the purpose of eliminate the mass-transfer limitation [54,55]. Table 1 shows the various advantages and disadvantages of suspended/slurry and immobilized/deposited photocatalytic reactors.

The spinning disc reactor as a photocatalytic reactor depicts important characteristics such as the reduction of mass transfer limitations as a result of the combination of thin liquid film and flow turbulence, which terminates to the increase of the mass transfer, acceptable and reliable product quality and the decomposition efficiency increases [63,64]. Therefore, in the last two decades (from 2000 until now), several studies have been concentered on the expansion of the spinning disc photocatalytic reactor, which has various

configurations (which rotate the disc horizontally and vertically) and further changes of the effective parameters such as flow rate, disc rotation speed, pH, the initial concentration of the pollutant, the type and intensity of light radiation and temperature have been investigated on the efficiency of photocatalytic reactions, especially in water environments (water and wastewater treatment) [51,52,65]. Two major various spinning disc reactor configurations were examined in the published articles as vertical and horizontal discs models. The vertical reactor configuration implies that the lower half disc is immersed in the liquid or fluid and bringing the upper half of the liquid to its surface and is exposed to the light source [66]. In this study, the focus is on the horizontal spinning disc photocatalytic reactors on which the liquid is placed as a thin film layer and exposed to a light source.

In the SDR system, the quality of the pollutant removal/degradation process relies mainly on the hydrodynamic characteristics of liquid films and irradiation intensity. Three distinct zones are displayed in the rotational speed profile on a spinning disc; the injection zone, acceleration zone, and synchronization zone obviously demonstrated in Fig. 1 [67,68]. These films are featured as a surface film with a solid-liquid interface. The injection zone causes the liquid exiting the nozzle to be slowed down by viscous drag after hitting the disc. The rotation of the disc in the acceleration zone increases the speed of the radial flow due to the creation of centrifugal force. The third zone is the synchronization zone, where the liquid rotates close to the disc rotation speed and the liquid film flow behavior resembles the Nusselt model [69]. The principle of the SDR system is based on a thin liquid film layer that is formed on a spinning disc, and its size sometimes reaches from 20 to 300 μm [43,44,69]. The liquid film formed on the disc surface creates centrifugal and shear forces, one reason for which is the tangential and radial acceleration, and the other reason is the ratio of surface area to mass volume and heat transfer coefficient, which causes the liquid film to high micromixing and very good [69,70]. These characteristics are beneficial in types of reactions, such as catalytic reactions as homogeneous or heterogeneous are of high significance, because the quick loss of heat and the high micromixing improve the quality of the product. The micromixing is of special significance when the reaction time is of the same order as the mixing time, i.e. the reaction time is less than the mixing time. As a result, the reaction is carried out under heterogeneous conditions, which may lead to the production of unwanted side reactions or lower yields [71–73].

Initially, based on a patent from 1925, spinning disc reactors were commercially extended to intensification of gas-liquid reactions. Today, to increase the rate of heat and mass transfer, the spinning disc reactor is used with intensified technologies, which are established through the centrifugal forces generated in the thin liquid film layer by the rotation of the disc. The SDR configuration and properties change in performance of the needed process yield and reactant species to be extended. In general, the rotation speed of the disc changes from 100 to 5000 rpm and the diameter of the disc from 10 to 100 cm [66]. Depending on the particular application the disc surface can be smooth, unstructured, grooved and meshed. Also, the disc material in most applications is usually stainless steel, but it can be ceramic, glass, alumina, brass to boost heat transfer, and Teflon to reduce clogging problems. Operational temperature and pressure are in the ranges −4 to 572 °F and 14.5–145 psi, respectively, whilst fluid flow rate entering the SDR depends on disc properties and rotational speed [64].

Regarding the limitations mentioned in the two types of slurry and immobilized reactors, the spinning disc reactor is considered a suitable option for the degradation of pollutants in water environments due to the aforementioned advantages. This review systematic study will focus on the photocatalytic degradation in spinning disc reactor and the influencing factors including hydrodynamic characteristics (disc rotational speed and flow rate), pollutant concentration, reaction kinetics, pH, irradiation time, disc surface structure and disc diameter will be investigated.

2. Methods

2.1. Literature survey and search approach

The standard method of Reporting Items for Systematic Review and Meta-Analysis (PRISMA) was selected for the systematic review [74]. A comprehensive screening route to the decomposition of pollutants by horizontal spinning disc photocatalytic reactor in

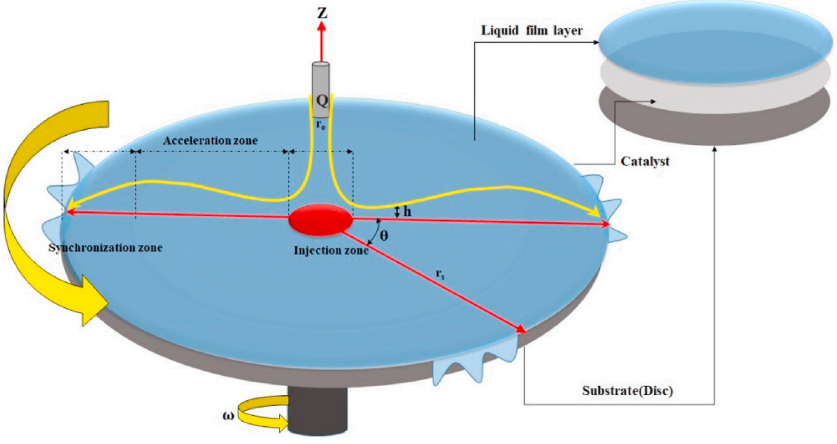

Fig. 1. Zoning of spinning disc photocatalytic reactor (injection zone, acceleration zone and synchronization zone positions).

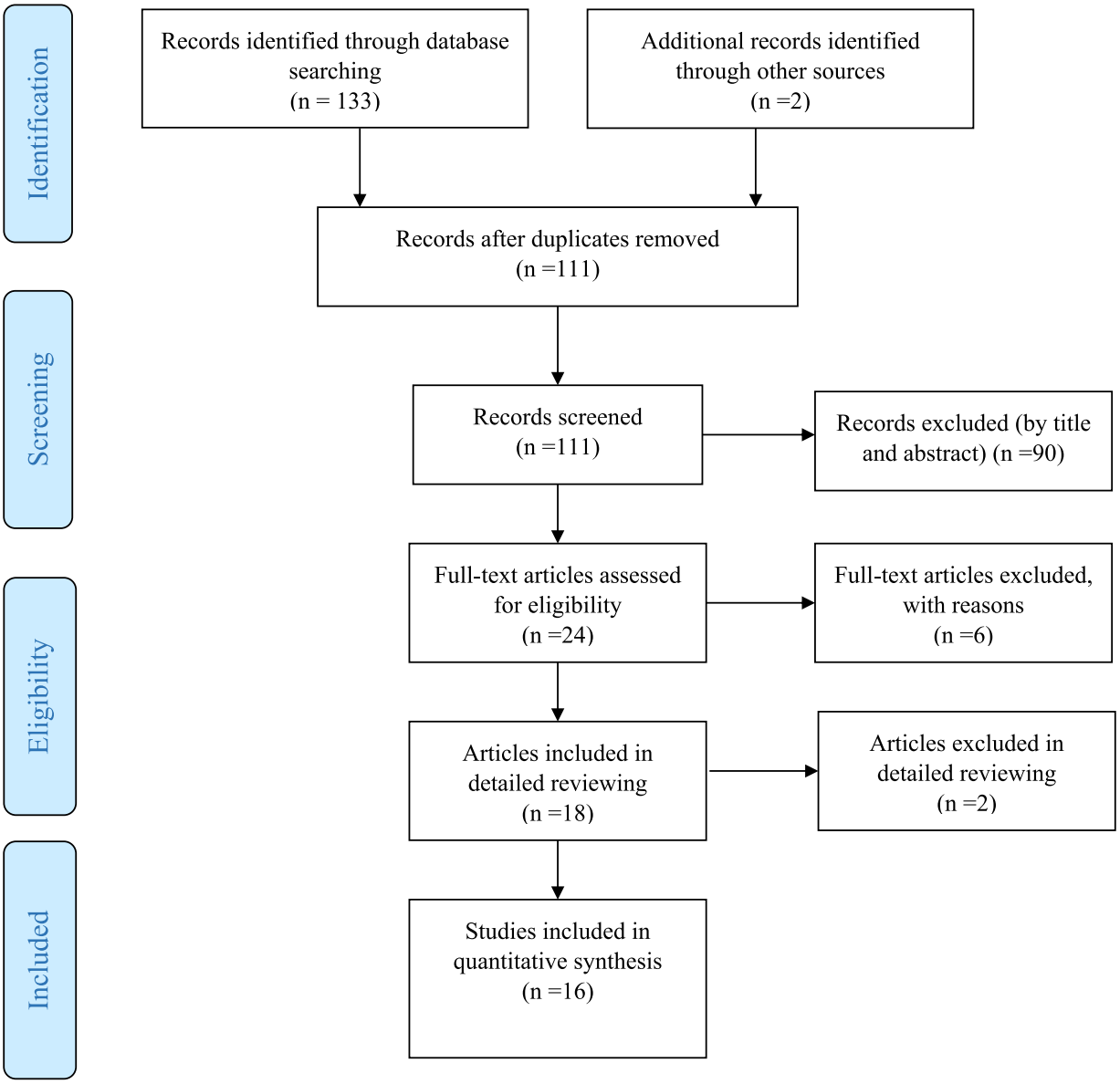

Fig. 2. Prisma study search and selection flow diagram.

aqueous environments within the documented literature was performed using Web of Science (WOS), Scopus, and Science Direct databases between January 1, 2001, and January 20, 2023. Once the papers from the mentioned databases were collected in the referencing administrator, the reduplicative records were eliminated, and a single record of each paper was retained. Afterward, the title, abstract, and full text of all papers were surveyed respectively. The search included the keywords ("Spinning disk reactor" OR "Spinning disc reactor" OR "Spinning disk photoreactor" OR "Spinning disc photoreactor" OR "Spinning disk photocatalytic reactor" OR "spinning disc photocatalytic reactor" OR "photocatalytic Spinning disk reactor" OR "photocatalytic Spinning disc reactor" OR "SDPR" OR "SDR" OR "pSDR" OR "Rotating Disk Reactor") AND ("Removal" OR "elimination" OR "degradation" OR "photo-degradation" OR "treatment") AND ("Photocatalyst" OR "photocatalysis" OR "photocatalytic" OR "photocatalyze") AND ("Water" OR "wastewater" OR "aqueous solution" OR "aqueous media"). The most appropriate papers were chosen based on the inclusion and exclusion criteria.

2.2. Inclusion and exclusion criteria

In this study, only original papers were selected that were published in English and peer-reviewed journals on the photocatalytic degradation of pollutants in SDR under light irradiation (UV and Visible light). In some studies rotator-stator spinning disc reactor (RSSDR) and vertical rotating disc reactor (VRDR) were investigated, so we selected the studies where spinning disc reactor had been

Table 2
Spinning disc reactor throughput and degradation efficiencies.

Catalyst	Synthetic route	Disc matter	Pollutant	Disc diameter (mm)	light source	Initial Conc.	Contact time	Light intensity	Kinetics order	Irradiant flux	Flow rate	Rotational speed	Efficiency	References
TiO_2	Sol-gel	Glass	Methylene blue	200	UV	8 mg/L	–	20 W	second order	13.9–22.9 w/m2	15 ml/s	–	–	[51]
TiO_2	Sol-gel	Glass	Methylene blue	200	UV	10 μmol/L	–	20 W	Pseudo-first-order	12-23 w/m2	15 ml/s	50–200	–	[44]
TiO_2(UV/H_2O_2/TiO_2)	Sol-gel	Glass	Antipyrine	200	UV	50	120 min	20 W	Pseudo-first-order	–	25	500	95.50 %	[48]
TiO_2	Sol-gel	Glass	Dehydroabietic acid	200	UV	5	–	–	–	–	–	–	–	[75]
TiO_2	Sol-gel	Glass	Methylene blue	200	UV	8	–	–	–	–	–	–		[75]
TiO_2	Dip-coating	Glass	Methyl orange	60	UV	4×10^{-5} M	–	2*4 W	first order	–	427 l/d	280 rpm	50 %	[54]
TiO_2	Sol-gel	Stainless steel	Phenol	190	UV	100	120 min	2*18 W	–	–	–	–	41 %	[76]
Fe–TiO_2	Sol-gel (dip-coating)	Stainless steel	Phenol	190	UV	100	120 min	2*18 W	–	–	–	–	70 %	[76]
TiO_2/H_2O_2	Sol-gel	Stainless steel	Phenol	190	UV	100	60 min	2*18 W	–	–	–	–	99 %	[76]
TiO_2	Dip-coating	Aluminium	Methyl orange	120	UV	4 × 10-5 M	–	2*4 W for each layer	first order	130–2760 mW/cm2	5 ml/min	–	96 %	[77]
TiO_2	Sol-gel	Stainless steel	Phenol	220	UV	30 mg/L	240 min	8*5 W	Second-order	–	2000 ml/min	290 rpm	100 %	[78]
TiO_2	Sol-gel	Stainless steel	Phenol	220	UV	30 mg/L	240 min	8*5 W	Langmuir-Hinshelwood	–	2000 ml/min	290 rpm	100 %	[79]
TiO_2	dip-coating	Teflon baffle 1	Phenol	220	UV	30 mg/L	180 min	8*5 W	Langmuir-Hinshelwood	–	–	150–225 rpm	100 %	[79]
TiO_2	dip-coating	Teflon baffle 2	Phenol	220	UV	30 mg/L	150 min	8*5 W	Langmuir-Hinshelwood	–	–	150 rpm	100 %	[79]
TiO_2 (Degussa P-25)	Immersed method	Glass	4-Chlorophenol		UV	91 μM	240 min	2*15 W	Langmuir–Hinshelwood	–	50 ml/s	350 rpm	near 0 μM	[80]
TiO_2(Tioxide PC1)	Immersed method	Glass	4-Chlorophenol		UV	91 μM	240 min	2*15 W	Langmuir–Hinshelwood	–	50 ml/s	350 rpm	<20 μM	[80]
TiO_2(Degussa P-25)	Immersed method	Glass	4-Chlorophenol		UV	91 μM	240 min	400 W	Langmuir–Hinshelwood	–	50 ml/s	350 rpm	<15 μM	[80]
TiO_2(Tioxide PC1)	Immersed method	Glass	4-Chlorophenol		UV	91 μM	240 min	400 W	Langmuir–Hinshelwood	–	50 ml/s	350 rpm	20 μM	[80]
TiO_2	Immersed method	Glass	Salicylic acid		UV	91 μM	240 min	2*15 W	Langmuir–Hinshelwood	27.9 W/m2	50 ml/s	350 rpm	<20	[80]
TiO_2	Immersed method	Glass	Salicylic acid		UV	91 μM	240 min	400 W	Langmuir–Hinshelwood	246 W/m2	50 ml/s	350 rpm	<10 μM	[80]
Ag/Ag_2O/TiO_2	sol-gel spin coating	Ceramic	Amoxicillin	200	LED	20 mg/L	80 min	5*6W	pseudo-first-order	11 mW/cm^2	0.6 l/min	225 rpm	97.91 %	[49]

(*continued on next page*)

Table 2 (*continued*)

Catalyst	Synthetic route	Disc matter	Pollutant	Disc diameter (mm)	light source	Initial Conc.	Contact time	Light intensity	Kinetics order	Irradiant flux	Flow rate	Rotational speed	Efficiency	References
TiO_2–P25 Nanoparticles	Ironing method	Polyethylene	p-Nitrophenol	275 mm	UV-C	15 mg/L	120 min	2*6 W	–	–	–	450 rpm	87.60 %	[81]
Bi_2O_3/Ag/TiO_2	sol-gel spin coating	Ceramic	Penicillin V	200	LED	30 mg/L	80 min	5*6W	Langmuir–Hinshelwood	11 mW/cm^2	0.8 l/min	180 rpm	97.67 %	[50]
B270 with Pt	PE-ALD	Glass	Ammonium	120	VL	2.3 mM	30 min	No mentioned	–	1574 w/m^2	89 ml/min	150 rpm	86.95 %	[82]
WO_3/Ag/ZnO S-scheme	Spray pyrolysis	Ceramic	Cephalexin	200	LED	40 mg/L	80 min	5*6W	Langmuir–Hinshelwood	11 mW/cm^2	1 l/min	180 rpm	98.8 %	[83]
Au–TiO_2	RF sputtering	Polycarbonate	Methyl orange	120	LED/UV	2 μM and 10 μM	90 min	34.2 μW/2*6W	–	–	6 ml/s	–	–	[84]

operated horizontally. These two types of reactors (RSSDR and VRDR) are not considered in this study due to their conditions and mechanisms. The inclusion criteria for qualified review were carried out as follows: Using any type of light irradiations, using any type of catalytic nanocomposites, conducting experiments in a horizontal spinning disc reactor as a photoreactor, and degradation of any types of pollutants or active substances. Finally, photocatalytic degradation in a horizontal spinning disc reactor was studied. Conference papers, reviews, abstract, the papers with duplicative content, irrelevant topics, books, presentations, and letters to the editor on pollutants degradation using SDR were excluded from the study.

2.3. Screening and criterion selection

Screening and criterion selection was done in four stages as follows:

1 Duplicate documents were removed using EndNote (version ×9) software.
2 The titles of the papers were evaluated by two autonomous reviewers and the studies were selected according to the main purpose of the current research.
3 The abstract of the formerly chosen studies were investigated and unrelated studies were eliminated from the scope of the research.
4 The full text of the studies selected based on the criteria was fully studied and reviewed.

The comprehensive data extracted from the selected documents were analyzed. This information included photocatalyst type, pollutant name, hydrodynamic effects (disc rotation speed, flow rate), pollutant concentration, contact time, pH, light source wavelength (UV and visible light), light intensity (UV and visible light), UV and visible light power, reaction kinetic, and pollutant degradation efficiency.

3. Results and discussion

3.1. Characteristics of literature

The flow chart of PRISMA based on the number of documents identified from different databases is shown in Fig. 2. All documents have been evaluated for eligibility according to the purpose of the study and the criteria mentioned. After reviewing the papers and removing duplicates, 111 documents were retained for further review based on the titles and abstracts. By selecting the papers based on the title and abstract in the previous stage, the full texts of 24 relevant papers were recaptured. Eventually, 16 papers were chosen based on the inclusion criteria of the study. The number of 2 photo-oxidative papers (removal of p-nitrophenol), 3 papers on color removal and 1 paper on photo-copolymerization, although the pollutant removal process has been investigated in SDR, it was excluded from the documents due to the lack of use of the catalyst deposition on disc surface in SDR.

3.2. Characteristics of the preserved papers

Table 2 summarizes of the photocatalytic degradation of various pollutants in the SDR based on publication in journals. Among the 16 papers, the sum up the number of studies conducted based on published journals was as follows: applied catalysis b: environmental (n = 1), chemical engineering journal (n = 2), Chemosphere (n = 2), Journal of Environmental Management (n = 2), Applied Sciences (n =), Journal of Photochemistry and Photobiology A: Chemistry (n = 1), Industrial and Engineering Chemistry Research (n = 2), Environmental Science and Pollution Research (n = 1), Modern Chemical Industry (n =), Journal of Chemical Engineering of Japan (n = 1), Catalysis Communication (n = 1), Optical Review (n = 1), Optics Express (n = 1), Environmental Technology (n = 1).

Based on the type of pollutant, 6 papers on dyes degradation, 3 papers on pharmaceutical compounds degradation, 2 papers on acid removal, 5 papers on phenols removal (3 papers on phenol removal, 1 paper on nitrophenol removal, and 1 paper on chlorophenol removal) and 1 paper on ammonia removal in spinning disc photocatalytic reactors have been investigated. Based on the type of light irradiations, 11 papers on UV irradiation, 4 paper on visible light irradiation (LED) and 1 paper on dual irradiation (LED/UV) have been investigated. Based on the type of catalyst nanocomposites used on the disc surface, 9 papers on TiO_2 catalyst alone, 6 papers on composites with TiO_2 as one of its catalysts immobilized on the disc surface have been investigated (see Table 2).

Table 3
Variation of the value of k_1 and k_2 (reaction constants within eq.) with lamp type used and radiation intensity for the degradation of 4-chlorophenol and salicylic acid [80].

Pollutant	Lamp type used	UV intensity (W/m^2)	k_1 ($dm^3/\mu M$)	k_2 ($\mu M/min$)
4-chlorophenol	LP	14.0	0.0507	6.25
	LP	27.9	0.0439	7.24
	MP	27.9	–	2.53
	MP	49.0	–	2.72
	MP	98.2	0.0562	4.23
	MP	240	0.0505	4.64
Salicylic acid	LP	27.9	0.0562	4.65
	MP	246	–	3.11

3.3. Modeling in spinning disc photocatalytic reactor (SDPR)

In explaining the modeling and kinetic analysis of photocatalytic reactions, it should be noted that heterogeneous photocatalysis is principally based on the kinetics of the Langmuir-Hinshelwood type (L-H), which can be linear or mixed linear and square root and depends on the light intensity [85,86]. The main problem in this type of kinetics is the use of reaction rate with mean light intensity, and it can only be valid when the reaction rate measures linearly with the light intensity at any point of the reaction position in the reactor [32]. The reaction kinetics in the photocatalytic degradation of pollutants depends on the reactor geometry, dimensions, irradiation sources, illuminations, flow conditions, hydrodynamics (turbulent and laminar flow type, batch, continuous, semi-continuous, rotation) and hydrodynamic factors (disc rotation speed in SDRs and flow rate) [87].

3.3.1. Reaction kinetic modeling in SDPR

In reaction kinetics, one of the important factors influencing the reaction rate and pollutant degradation efficiency is the reaction rate constant. In most researches, the kinetic rate constant is dependent on the effects of mass transfer in the reactor. Reaction rate constants are reported to be different due to mass transfer effects. These effects have been investigated according to the volume of liquid inside the reactor, stirring speed, disc rotation speed, light intensity, etc [88–90]. The effective rate constant is higher in high-volume reactors than in low-volume reactors, which indicates that the overall reaction occurs faster. It is remarked that an increase in the initial concentration of the pollutant leads to a decrease in the degradation rate. The reason is that the active sites of the catalyst with higher pollutant concentration and light scattering affect the route of induced photons [90].

3.3.2. Most of the reaction kinetics in SDPR follow the Langmuir-Hinshelwood model (Eq. (1)). In this model

$$-r = -V_l\frac{dC}{dt} = \frac{k_1 k_2 C}{1 + k_1 C} \tag{1}$$

wherein.

V_l = the volume of treated liquid

k_1 = the absorption equilibrium constant for the reactant species

k_2 = the reaction rate constant.

C = the concentration of pollutant

t = the time of reaction (min).

It can be stated that k_2 illustrates the restricted rate of pollutant reaction, while k_1 is related to the pollutant absorption with the catalyst surface that is proportional to the intensity of the incident photon at the catalyst surface.

As soon as the light radiation is transmitted to the liquid film on the disc surface, the contaminant absorption in the film occurs. The pollutant adsorption process in the liquid film is described by the Beer-Lambert equation (Eq. (2)) [54,77].

$$\varepsilon hC = -\log\frac{I}{I_o} \tag{2}$$

wherein.

ε = molar absorptivity.

I = light intensity at the bottom of the liquid film.

I_o = light intensity at the surface of the liquid film.

Substituting Eq. (2) into Eq. (1) gives Eq. 3

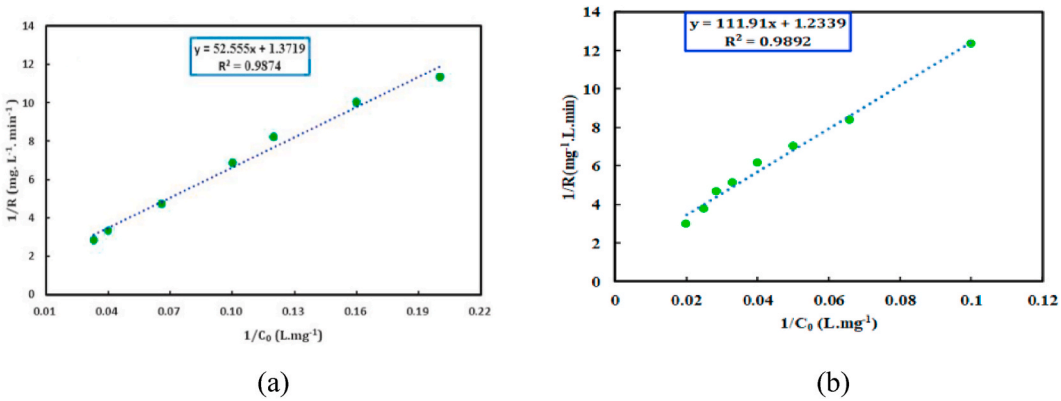

Fig. 3. The reaction kinetic models for the photocatalytic degradation of Amoxicillin (a) [49] and Cephalexin (b) [83].

$$-r = -aI_o k_1 \exp(-\varepsilon hC)\frac{C}{1+k_1 C} \quad (3)$$

Yatmaz et al. investigated the kinetics of the reaction based on Langmuir-Hinshelwood kinetics (Eq. (3)) for radiation intensity. In their work, TiO_2 catalyst was deposited on a glass disc, and UV lamp with low (LP) and medium (MP) pressures were used as a source of radiation to degrade two pollutants (4-chlorophenol and salicylic acid). Table 3 shows the results of experiments to evaluate the effect of UV radiation intensity and wavelength on the reaction rate. The results showed that doubling the intensity of UV radiation with low pressure for the degradation of 4-chlorophenol was significant, but it had little effect on limiting the reaction rate or k_2. However, the value of k_1 or the absorption equilibrium constant for reactant species when exposed to different radiation intensities, did not show a significant effect [80]. Yatmaz et al.'s reason was that the change in the k_1 value was caused by experimental error instead of the real value. They also could not calculate the value of k_1 in the intensity of the lower medium pressure lamp due to the compliance of the degradation rate of the pollutant to zero-order. The values of k_1 and k_2 for the degradation of salicylic acid followed zero-order kinetics in the case of medium-pressure lamps and mixed kinetics for low-pressure lamps. Since the value of k_2 depends on the amount of coated catalyst in the SDR reactor, it can affect the radiation intensity and degradation efficiency. Therefore, the comparison of Yatmaz et al.'s study with other studies showed that the catalyst coating technique used in this study was not sufficient for SDR and reported that a supported catalyst with better mechanical properties is needed. The results of the experiments depicted different k_1 values in SDR. These values can be attributed to the production of a very turbulent liquid film, which increased the transfer rate of organic substances to the catalyst film [80].

Mirzaei et al. obtained different adsorption coefficients in different concentrations of phenol. They obtained k_1 coefficient for initial phenol concentrations of 30, 50, and 70 mg/l as 17.493, 0.06, and 0.008 L/mg and for k_2 as 0.062, 0.074, and 0.097 mg/s.L, respectively. At higher concentrations, more phenol molecules were adsorbed on the surface of the TiO_2 catalyst in the SDR system and causing competition between pollutant molecules and reaction intermediates for adsorption in the active sites of the TiO_2 catalyst. In general, the increase in the initial concentration of the pollutant led to an increase in the amount of adsorbed phenol molecules, which result in a decrease in the contact between the molecules and the active sites of the catalyst, and finally caused a change in the equilibrium of adsorption and relative coefficients [78].

Zamani et al. investigated the kinetics of the reaction under the optimal conditions of irradiation time of 80 min, initial concentration of amoxicillin of 20 mg/l, flow rate of 0.8 L/min, disc rotation speed of 225 rpm, pH = 6 and aeration speed of 20 L/min. They obtained the Langmuir-Hinshelwood (L-H model) rate and adsorption constants of 0.729 mg/min. L and 0.0261 L/mg, respectively (Fig. 3-a) [49]. In another study for photocatalytic degradation of cephalexin in an SDR system, they calculated photocatalytic reaction rate, Langmuir-Hinshelwood rate and absorption constants as 0.0456 1/min, 0.81 mg/min. L and 0.011 L/mg, respectively (Fig. 3-b) [83].

3.3.3. *Modeling the passed flow of the disc in SDPR*

Considering that the disc rotational speed and flow rate are different in the SDRs, the reactor must be modeled to contrast the kinetic rate constants between the work cycles. In reaction kinetic modeling, the overall reaction rate can be obtained by considering the concentration of catalyst and oxidant, light absorption rate, and mass transfer rate. It is also possible to calculate the mass balance in the reactor and the reservoir containing the pollutant as separate control volumes in SDR systems [44,75]. In the modeling of this system, it is assumed that the reactant tank behaves as an entirely mixed and ideal continuously stirred tank where the output concentration is equal to the tank volume concentration (Eq. (4)). Therefore, the variation of concentration in the tank with respect to time is calculated from differential equation.

$$\frac{dC_{inlet}}{dt} = \frac{Q}{V_{CST}}(C_{outlet} - C_{inlet}) \quad (4)$$

wherein.

C_{inlet} = the pollutant concentration in the tank and SDR input.

C_{outlet} = the SDR output concentration and tank input.

Q = the volumetric flow rate.

V_{CST} = the volume of the tank.

To modeling the reaction rate in the reactor, the total degradation rate of the pollutant solution is used. SDPR modeling requires that the fluid volume across the spinning disc be determined. In order to predict the liquid thickness across the disc surface, the Nusselt model presented in Eq. (5) is used, through which the SDPR volume can be calculated. This model presumes quite expanded laminar flow throughout the disc surface with no shear [69].

$$h = \sqrt[3]{\frac{3Q\vartheta}{2\pi r^2 \omega^2}} \quad (5)$$

Wherein h is the liquid film thickness at radius r on the disc, Q is the volumetric flow rate, ϑ is the kinematic viscosity of liquid, and ω is the rotational speed. For simplicity, all of the constants are integrated into a single variable α (Eq. (6)).

$$h = \alpha r^{-2/3} \quad (6)$$

To achieve mass balance, it is assumed that the SDR behaves as a plug-flow reactor. Therefore, the following differential equation is

obtained for the change of pollutant concentration on the substrate with respect to the radius across the disc.

$$\frac{dC}{dr} = 2\pi\left(\frac{3\vartheta}{2\pi Q^2\omega^2}\right)^{\frac{1}{3}} Rr^{\frac{1}{3}} \tag{7}$$

wherein.

R = the volumetric rate of reaction

r = the radius of disc.

According to Eq. (8), most of the reaction kinetics are second-order and this is unusual for photocatalytic reactions. For the photocatalytic reactions of the first order reactions, the Langmuir-Hinshelwood simplified kinetic expression is due to dilute pollutant concentrations [91,92].

$$R = k_\vartheta C^2 \tag{8}$$

Substituting Eq. (8) into Eq. (7) and integrating between the input and output radius (R_{inlet} and R_{outlet} respectively) equation (9) for the reaction across the SDR is obtained:

$$C_{outlet} = \frac{1}{2\pi k\left(\frac{3Q\vartheta}{2\pi\omega^2}\right)^{\frac{1}{3}}\left[R_{inlet}^{4/3} - R_{outlet}^{4/3}\right] + \frac{1}{C_{inlet}}} \tag{9}$$

Another factor expressing the reaction kinetics is surface area or volumetric in heterogeneous photocatalysis with a catalyst deposited on a substrate, where the surface area used is the irradiated surface, not the surface area of the photocatalyst. Surface reaction rate constants are carried out for comparative purposes because the effect of various reaction volume per surface area under various flow conditions and disc rotation speed on a SDR can be eliminated [75]. As a result, the reaction merely takes place on the surface of the spinning disc, and the surface rate constant can be expressed from the volume rate constant using Eq. (10).

$$k_s = \frac{V}{S}k_v \tag{10}$$

where.

k_s = the first or second order surface reaction rate constant

k_v = the first or second order volume reaction rate constant.

S = the irradiated surface area of the photocatalyst.

V = the volume of the reactor.

3.3.4. Flow modelling pass the disc

To model the flow across the disk in the SDR system, the film thickness distribution should be clear, and for this, the Nusselt model is the most widely used. In this model, it is assumed that the flow is completely laminar across the surface of the disc without shear at the gas-liquid interface. As mentioned in Eq. (5), the average film thickness can be calculated by the Nusselt model. The Nusselt model overpredicts the film thickness and cannot represent the surface waves [44]. To investigate the deviation of the film thickness from the Nusselt model, it can be approximated with the Ekman number. Ekman's number (E) is defined as the ratio of viscosity forces to coriolis forces and is expressed by Eq. (11):

$$E = \frac{\vartheta}{\omega h^2} \tag{11}$$

In this equation, when the Ekman number is greater than 10, the film thickness can be approximated by the Nusselt model. But for low values of Ekman number, the inertial forces overcome and the film thickness significantly deviates from the Nusselt model [69,93].

Table 2 lists the selected results of catalyst-based SDR for pollutants removal published in the last two decades. In all studies performed so far batch and continuous reactors have been usually used for pollutants removal of spinning disc photocatalytic reactor, including phenol, chlorophenol, dyes (e.g. methylene blue, methyl orange) and drugs (e.g. antipyrine, penicillin V, Ciprofloxacin and amoxicillin) [44,48,49,76,78,79].

3.4. Effective factors on the performance of SDPR

In the documents presented in this systematic review article, the effect of one or more factors on pollutant degradation or SDR performance has been investigated. Therefore, some factors considered in the discussion may not be comparable. In other words, due to the challenges and gaps in the photocatalytic performance of SDR, some factors that have not been investigated by previous researchers or need further data have been experimented and investigated by new researchers.

3.4.1. Effect of radiation intensity and photonic efficiency

As respects photocatalytic processes need the attendance of an active catalyst and light illumination in order to accelerate the reaction, limitations of mass transfer and photon transfer are the two main and definite limitations for achieving these types of

processes on an industrial scale [94,95]. Due to these two limitations, slurry-type reactors, spinning discs and microreactors have shown significant performance in solid/liquid systems [94]. Because photocatalytic reactions caused by light radiation are mostly carried out in liquid environments, therefore the most contact between the photocatalyst and the pollutant occurs in the liquid solution. Although research work has been done in this field, more research is still needed to achieve industrial scale [95]. Among the various reactors designed so far for photocatalytic performance, spinning disc reactors and microreactors to maximize reactant mass transfer to the catalyst's active surface showed the highest coating surface with catalyst per volume of the reaction liquid. In other words, it represents the amount of illumination surface per unit volume of the reactive liquid solution inside the reactor [94]. In this case, Gorges et al. observed the highest catalyst coating surface area per reactive liquid solution volume of 12,000 m^2/m^3 for their microreactor, while Van Gerven et al. reported a much higher catalyst-coating surface area per reaction liquid volume (20,000–66000 m^2/m^3) for the spinning disc reactor system [94,96].

The photonic efficiency in photocatalytic degradation can be defined by the overall quantum yield in terms of moles of reacted substrate per absorbed photon. Since it is difficult to determine the rate of photon absorption, so the photonic efficiency was used as an alternative (Eq. (12)) [97].

$$\varphi = \frac{R_d}{J_f A} \times 100 \tag{12}$$

wherein.

φ = photonic efficiency

R_d = initial degradation rate (mol/s).

J_f = photon flux (mole photons/m^2s).

A = the surface area of the rotating disc radiation (m^2).

The photon flux (J) can be determined by.

To calculate the photon flux (J_f), Planck equation is used to determine the energy of 1 mol of photon and convert the measured radiation from light radiation to photon flux (Eq. (13)).

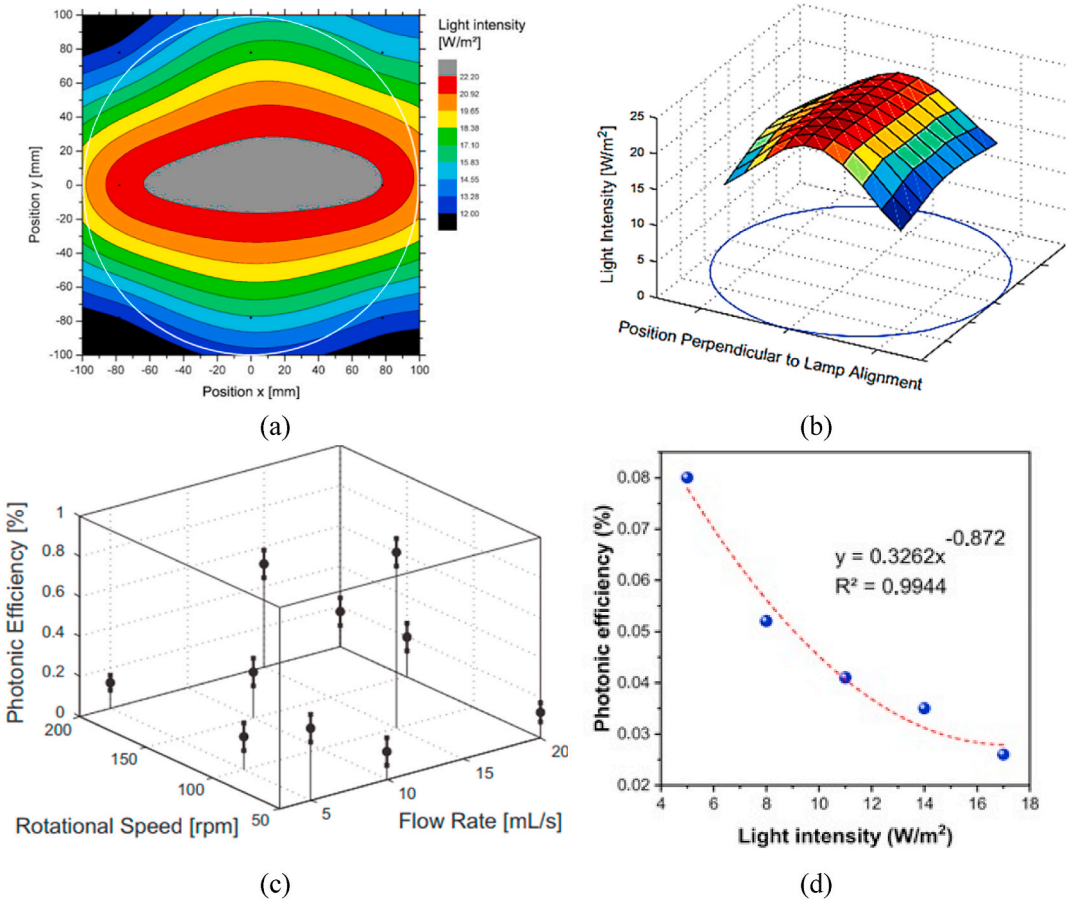

Fig. 4. **(a)** Irradiation profile inside spinning disc reactor [44] (b) and (c) effect of radiation intensity and photonic efficiency [51] and (d) effect of light intensity on the photonic efficiency [83].

$$E_p = \frac{hc}{\lambda} N_A \tag{13}$$

$$J_f = \frac{I}{E_p} = \frac{I\lambda}{hcN_A} \tag{14}$$

wherein.

E_p = Photon energy (J/Einstein).

h = planck's constant (6.626×10^{-34} J s).

c = the speed of light (3×10^8 m/s).

λ = the wavelength of the light (m).

N_A = Avogadro's constant (6.023×10^{23} photons/mole).

I = the incident light intensity (W/m^2).

According to equation (14), the photon efficiency is determined by dividing the pollutant photocatalytic degradation rate by the photon flux. This means that the number of pollutant molecules degraded is related to the number of photons that have incident from the light source. The photon efficiency changes during the photocatalytic process in SDR according to the changes in the pollutant concentration inside the reactor and causes a change in the reaction rate (Eq. (15)).

$$R = \frac{(C_o - C_t)V}{M_w t} \tag{15}$$

wherein.

R = the reaction rate.

C_o = the initial pollutant concentration (mg/L).

C_t = the reactant content at the time of t (mg/L).

V = the reactor volume (L).

M_w = the molecular weight of pollutant (mg/mole).

t = time of reaction.

Finally, to fit the photonic efficiency in the reactor, the experimental relationship based on the power law model (Eq. (16)) is used.

$$\varphi = \alpha I^{\beta} \tag{16}$$

where α and β are constant values that are obtained based on the experimental conditions and give the best fitting model.

Zamani et al. investigated the effect of radiation intensity on photon efficiency for the degradation of cephalexin antibiotic using an LED lamp. From Eq. (12), they obtained the best fit of the photonic efficiency in the SDR reactor. In Fig. 4(a–b), the range of radiation intensity is 5–17 mW/cm^2 and LED photon flux is 1.94×10^{-4}-8.61×10^{-5} E/m^2. s. The photonic efficiency has reached from 0.08 % at the radiation intensity of 5 mW/cm^2 to less than 0.03 % at the radiation intensity of 17 mW/cm^2. At higher photon flux, WO_3/Ag/ZnO S-scheme photocatalytic composite absorbed higher photons, which will lead to the generation of more electron-hole pairs. They also reported that the initial apparent photon efficiency was lower at high photon fluxes compared to low photon fluxes. The reason for this is the lower use of light energy at high photon fluxes [83].

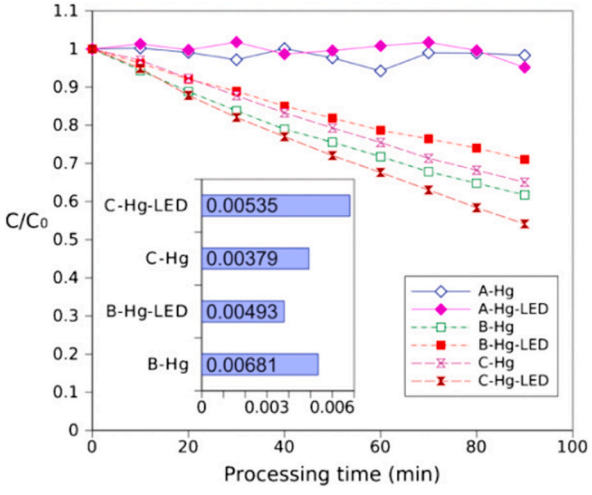

Fig. 5. Methyl orange degradation by the irradiation of red LED lamp (visible light) and Low pressure mercury lamp (UV) for PC/TiO_x (sample A), PC/TiO_x/TiO_2(sample B), and PC/TiO_x/Au–TiO_2 (sample C) discs [84]. (For interpretation of the references to color in this figure legend, the reader is referred to the Web version of this article.)

The UV radiation measurements in SDR at disc surface were performed by Boiarkina et al. [51]. They performed this measurement in a 3*3 grid arrangement with a total of 9 points, with each measurement repeated three times at each location, before and after the experiments. The results of before and after measurements showed that were consistent in the margin of error (MOE), so the mean of the two profiles was used to calculate the irradiation flux on the surface of the spinning disc, shown in Fig. 4. The maximum radiation of the lamp occurs at 22.7 ± 2.9 W/m^2 at the central axis, which is aligned with the lamp. In this research, the heterogeneous nature of the radiation profile was reported to be undesirable for modeling the SDPR, because depending on the radiation flux at that stand, there is a local change in the reaction rate on the disc surface [51]. The maximum radiation flux obtained was more than 1.5 times the minimum (13.9–22.9 W/m^2), which was more homogeneous compared to the study by Dionysiou et al. [52]. They reported that the mean photon flux reaching the catalyst surface at SDR was $3.99 \times 10^{-5} \pm 5.1 \times 10^{-6}$ E/m^2. s [51]. The results showed that in the initial concentration of methylene blue (8 mg/l) and in half of the initial concentration, the average photonic efficiency was 0.19 ± 0.08 % and 0.05 ± 0.02 %, respectively. The overall maximum photonic efficiency was obtained at a flow rate of 15 mL/s and a rotation speed of 100 rpm for the initial concentration of methylene blue and at half of the initial concentration of 0.88 ± 0.07 % and 0.44 ± 0.02 %, respectively [51].

In another study conducted by Boiarkina et al. the radiation intensity was calculated as 12–23 W/m^2. The results of their work depicted that UV radiation is the most uniform radiation for SDPR. The reason for that is the parabolic mirror used with the UV lamp with relatively uniform radiation on the disk surface. The photonic efficiency is presented in Fig. 4(c–d) according to the disc rotation speed and flow rate [44].

3.4.2. *Effect of a dual light source on the pollutant degradation*

Light is divided based on wavelength to visible light and nonvisible light. Visible light wavelength is 400–700 nm. Nonvisible light is divided into ultraviolet (UV) light (wavelength< 400 nm) and infrared light (wavelength >720 nm). The visible wavelength range starts from violet light (400 nm) with a wavelength close to UV light and continues to red light (700 nm) with a wavelength close to infrared light [98,99]. The photocatalytic reaction rate depends on the intensity of the incident light achieving the catalyst surface. Therefore an exact designation of the local light flux striking the catalyst surface is required. Photocatalytic reactors are naturally irradiated by UV/visible lamps that are located at an optimum distance to the catalyst film for maximum reaction [98,99].

Huang et al. evaluated the effect of a dual light source including two types of visible (red LED; 637 nm, 34.2 μW) and ultraviolet (Low pressure mercury; 254 nm) lamps in the absorption of methyl orange by three types of catalytic compounds in the circular plate waveguide of a spinning disc reactor [84]. They used a polycarbonate (PC) disc with three deposited thin film catalytic compounds of PC/TiO_x, PC/TiO_x/TiO_2, and PC/TiO_x/Au–TiO_2 to compare the effect of two types of light source on the degradation of methyl orange. Flow rate 6 ml/s, pollutant concentration was considered for PC/TiO_x 2 μM as a reference and for PC/TiO_x/TiO_2 and PC/TiO_x/Au–TiO_2 10 μM and at a certain rotation speed. Fig. 5 depicts that the disc sample of PC/TiO_x has a low photocatalytic efficiency under mercury lamp irradiation, with or without red LED light (sample A at Fig. 5). The final concentration of methyl orange (C/C_o) for the disc sample of PC/TiO_x/TiO_2 with or without red LED (sample B) was 0.71 and 0.62, respectively, and for the disc sample of PC/TiO_x/-Au–TiO_2 with or without red LED (sample C), 0.54 and 0.65 were obtained, respectively. The photocatalytic efficiency of the Au–TiO_2 composite under the combined irradiation of UV light and LED light was approximately 24 % higher than the photocatalytic efficiency of TiO_2 under UV light alone. The reason for that was that the irradiation of the red LED lamp with a wavelength of 637 nm produced a plasmonic photocatalytic reaction on the composite Au–TiO_2 nanoparticles, which is associated with the Au plasmon element [84].

3.4.3. *Effect of disc surface structure on pollutant degradation*

The disc surface structure affects the pollutant degradation efficiency due to the creation of turbulence and mixing. The effect of disc surface structure on phenol degradation in aqueous media under optimal conditions of rotation speed = 290 rpm and flow rate = 2 l/min was investigated by Mirzaei et al. In this study, three types of smooth disc (Stainless steel), baffled discs type I and II (Teflon)

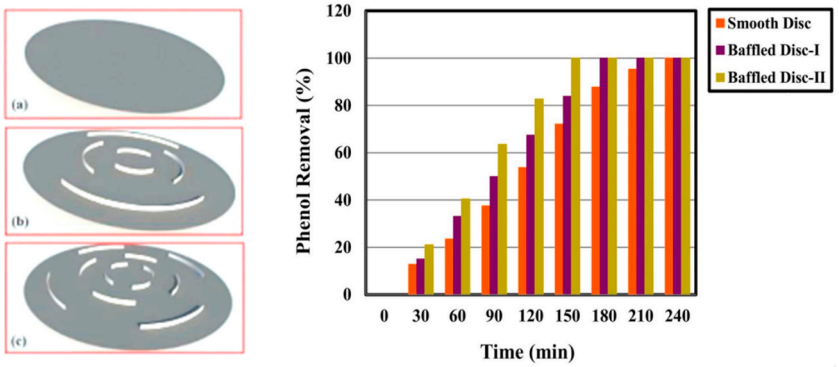

(a) (b)

Fig. 6. Different structures of disc surface (smooth, baffled disc I and baffle disc II) (a) and effect of disc surface structure on the pollutant degradation in SDPR (b) [79].

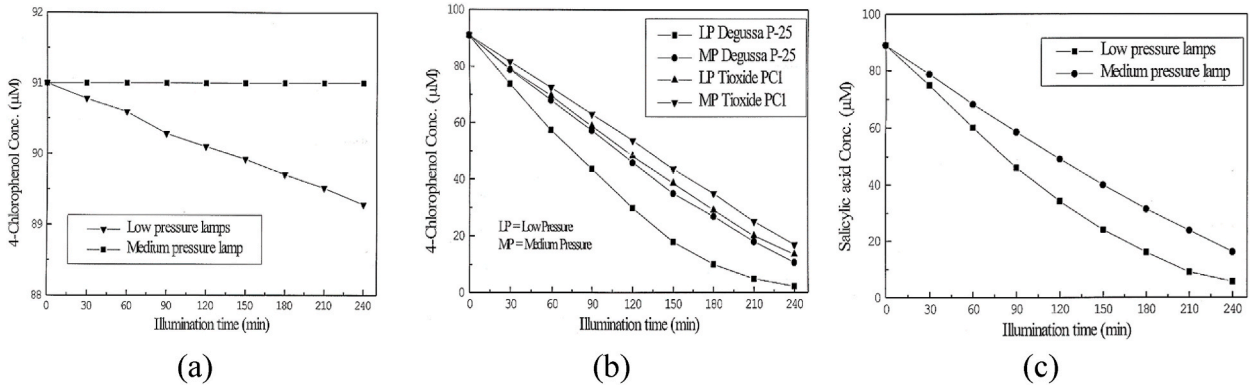

Fig. 7. Effect of lamp type (a) for 4-chlorophenol, (b) catalyst type and (c) for salicylic acid on the performance of SDPR [80].

were tested (Fig. 6-a). According to the results for these three discs, the complete degradation of phenol was at 240, 180 and 150 min, respectively (Fig. 6-b). The reason for complete degradation in a shorter period of time is the presence of baffle discs due to increased turbulence and as a result good mixing in the reactor [79]. Another reason for the results was residence time. This is because each baffle acts as a barrier to the liquid thin film, thus increasing the residence time under similar operating conditions. Finally, more pollutant solution remained in the reactor reaction zone and faster and better degradation was obtained [79]. Obviously, the surface of catalyst was the same for both baffled discs and the differences between their efficiencies related to the distinct embellishment of baffles. The presence of baffles creates barriers that enhance turbulence, leading to better mixing and shorter degradation times. Additionally, the residence time of the liquid thin film is increased due to the presence of baffles, allowing for more efficient degradation under similar operational conditions. Despite the catalyst surface being consistent across the baffled discs, the differences in their efficiency can be attributed to the unique design of the baffles. This study highlights the importance of disc surface structure in optimizing pollutant degradation efficiency within spinning disc reactors.

3.4.4. Effect of lamp type (UV and visible) on the degradation of pollutant

Yatmaz et al. investigated the effect of two types of mercury lamps, low pressure (15 W, 254 nm) and medium pressure (400 W, 365) on the degradation of 4-chlorophenol and salicylic acid in photocatalytic studies in a SDPR. The catalyst used was titanium dioxide (Degussa p-25). Their best results were obtained when a low pressure lamp was used (Fig. 7-a). They used the full output power of a medium pressure lamp but the results were better in low pressure lamp conditions. This could be due to the photochemical reaction at the wavelength emitted by low pressure lamps. However, little photochemical decomposition occurred when the 4-chlorophenol solution was irradiated with low pressure lamp without the presence of a catalyst, but no photochemical decomposition occurred in medium pressure lamps. They eventually concluded that the improvement in the performance of low-pressure lamps was due to its photocatalytic nature [80]. Also, two types of catalysts (TiO_2, Degussa p-25 and Tioxide, PC1) with the mentioned conditions in two types of lamps were examined. Their results showed that in both types of lamps, a higher degree of degradation of organic matter was obtained in the Degussa p-25 catalyst (Fig. 7-b). To evaluate the type of catalyst and lamp, the performance of the SDPR was examined by salicylic acid (Fig. 7-c). According to Fig. 7-c., the low pressure lamp again produced a higher photocatalytic behavior and it was found that the photocatalytic effect of the low pressure lamp is independent of the nature of the organic compound [80].

3.4.5. Effect of pH on the degradation efficiency of pollutant

The pH is a variable controlling the charges of catalyst and pollutant, adsorption effectiveness of pollutant on the catalyst surface and further give an effect on the degradation efficiency [15]. In general, the effect of pH on the degradation of pollutants in spinning disc photocatalytic reactors has not been investigated. Zamani et al. studied the effect of pH on the efficiency of photocatalytic degradation using the $Ag/Ag_2O/TiO_2$ thin film catalytic compound in the range of 2–10 as shown in Fig. 8-a [49] and Table 2. They found that the degradation efficiency of Amoxicillin by SDR was increased by decreasing the initial pH of the solution. The reason was firstly the production of hydroxyl radicals as a result of oxidation of hydroxyl ions, secondly the process of hydrolysis of amoxicillin at high pH, due to the instability of the β-lactam fraction of antibiotics [49,100]. The best performance was achieved in weak acidic conditions with pH = 6. In another study on the degradation of antipyrine drug using $UV/H_2O_2/TiO_2$ heterogeneous in SDR, the highest rate of degradation was obtained in pH = 4 and H_2O_2 = 1500 mg/l (Fig. 8-b) [48]. Huang et al. studied the pH changes in ammonium oxidation by SDR in the presence of visible light with plasmonic photocatalytic enhancement (Fig. 8 c-d). For this, they used a modified soda-lime glass substrate with or without a platinum film (B270 glass substrate with or without Pt thin film) [82]. In another study by Zamani et al. when $WO_3/Ag/ZnO$ S-scheme composite was used to coating the disc surface as a photocatalytic thin film, the degradation of cephalexin was experimented at pH between 2 and 10 and irradiation time of 20–100 min (Fig. 8-e). According to Fig. 8-e, they obtained the maximum efficiency of cephalexin degradation at pH = 6. The reason for this degradation efficiency is reported to be the interaction between the active sites of the photocatalytic composite and cephalexin molecules. Also, increasing the time of light irradiation due to prolonging the contact time of the pollutant with the photocatalyst surface has led to more free radicals and as a result, increased degradation efficiency [83]. Therefore, pH can play a very important role in the photocatalytic degradation of

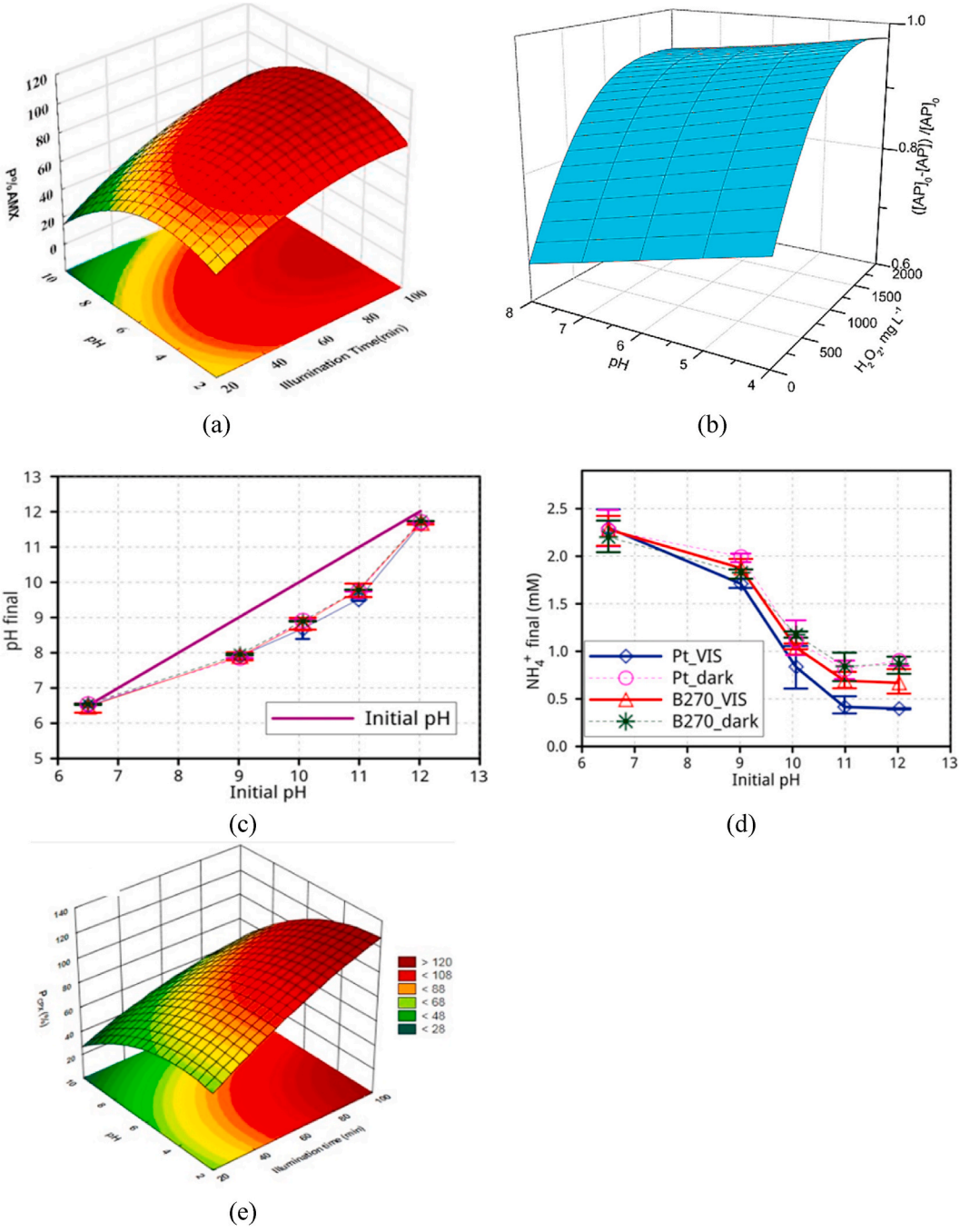

Fig. 8. Effect of pH on the pollutant degradation in SDPR for amoxicillin (a) [49], antipyrine(b) [48], various initial pH levels on the final pH for NH_4^+ oxidation(c), various initial pH levels on the oxidation of NH_4^+(d) [82] and for cephalexin(e) ([83]).

pollutants and controlling adsorption on the catalyst surface.

3.4.6. Effect of hydrodynamic factors (rotation speed and flow rate)

Two very important hydrodynamic factors in spinning disc photocatalytic reactors is the rotation speed of the disc and the flow rate, which has a significant effect on the degradation efficiency of pollutants and the performance of SDPR [51,101]. One of these hydrodynamic factors is the rotational speed of the disc, which can be investigated with an extra degree of freedom in the control of spinning disc photocatalytic reactors, because the mixing intensity, residence time and degradation/conversion efficiency, may be controlled by modifying the rotational speed, instead of more common methods used of varying flow rates [102]. Mirzaei et al. by

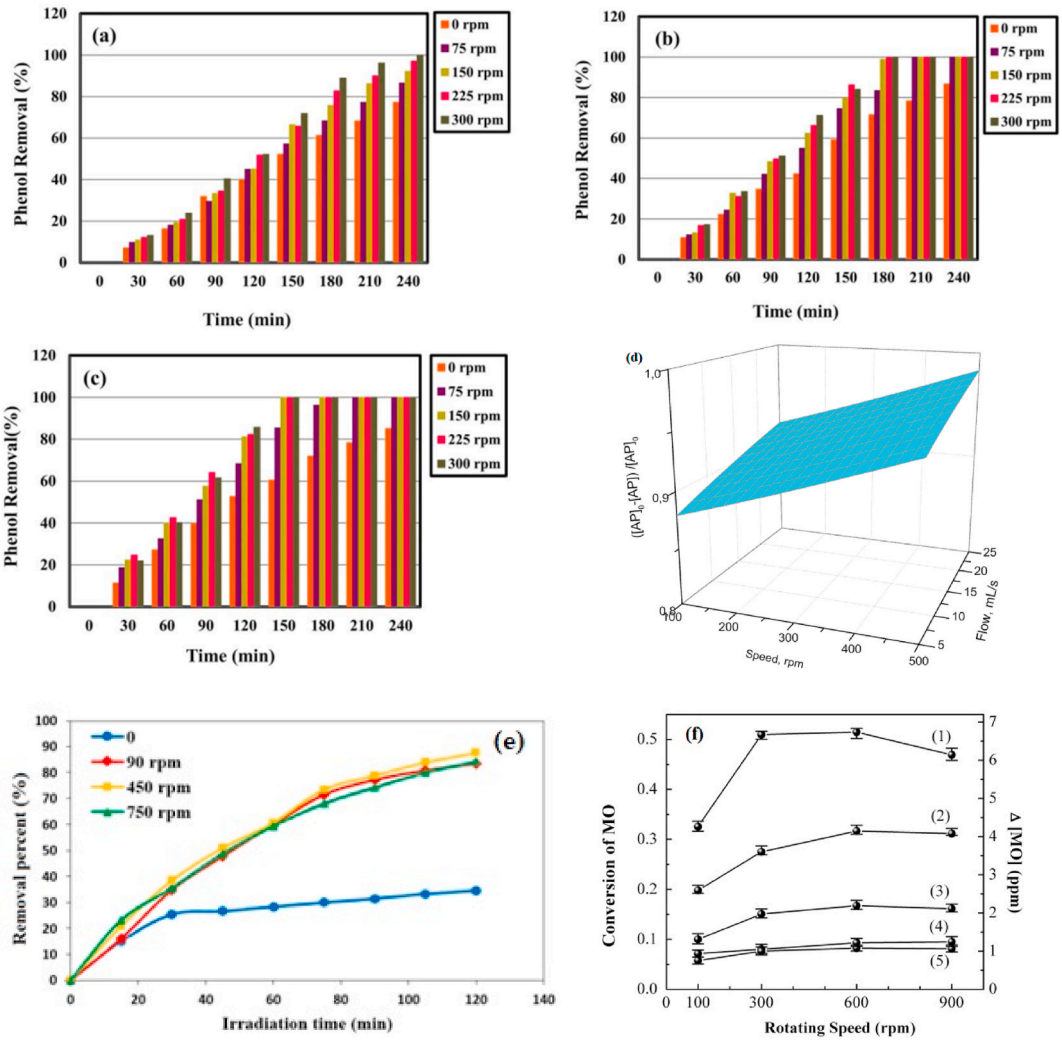

Fig. 9. Effect of disc speed on the pollutant degradation in SDPR for phenol (a-Smooth disc, b-Baffled disc I and c-Baffled disc II) [78,79], antipyrine (d) [48], PNP(e) [81] and methyl orange(f) [54]. (For interpretation of the references to color in this figure legend, the reader is referred to the Web version of this article.)

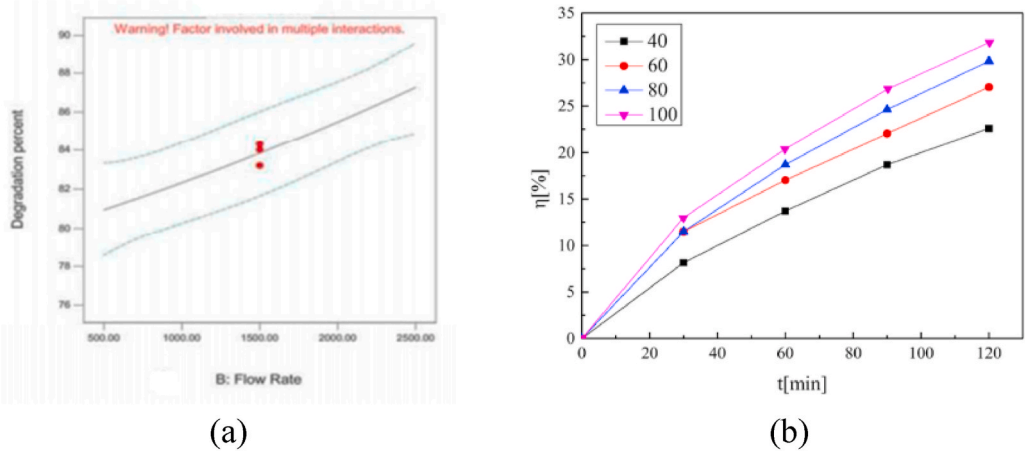

Fig. 10. Effect of flow rate on the phenol degradation [76,78].

examining the rotational speed of the disc on two types of smooth and baffled disc, showed that when the disc rotation speed increases from 0 to 300 rpm in smooth discs, the amount of phenol removal increased from 78.3 % to 100 % within 4 h reaction time [79]. For baffled discs, the highest disc rotation speed to reach the highest efficiency was 150 rpm. They explained that at disc rotation speeds above 150 rpm, phenol removal does not increase significantly because baffled discs create turbulence and agitation and improve mass transfer properties (Fig. 9-a-c). Therefore, above the critical rotation speed, the reaction rate is limited by surface and kinetic reaction and not by mass transfer. This means that the new discs influence on mass transfer and kinetic is explicit, but a higher critical rotational speed reaction is controlled by reaction kinetics [79,103,104]. Exposito et al. investigated the removal of antipyrine drug compound at 100–500 rpm of disc rotation speed. Their results showed that the highest rate of antipyrine degradation occurred at a rotation speed of 500 rpm (Fig. 9-d). Their justification for increasing the destruction of antipyrine was to improve mass transfer due to extra effect of oxygen into reactor through water-air interface on the thin film of antipyrine solution of spinning disc [48]. Behnajady et al. investigated the percentage of p-nitrophenol (PNP) photodegradation using TiO_2–P25 thin film at horizontal spinning disc reactor as a function of disc rotation speed. They indicated for initial PNP concentration of 15 mg/L and solution pH of 5.5 increased PNP photodegradation efficiency with increasing disc rotation speed to 450 rpm and afterward starts to decrease. The decrease in efficiency was reported below the optimal speed of the disc rotation due to the thickness of the PNP solution film on the disc surface, and above the optimal speed was due to the reduction of the residence time (Fig. 9-e) [81]. Chang and Wu depicted in Fig. 9-f that the photodegradation rate of methyl orange is a function of the disc rotation speed for different flow rates (3, 5, 10, 20 and 25 mL/min). For a constant flow rate, the degradation of methyl orange increased with increasing rotation speed, but it decreased when the rotation speed of the disc was higher than 600 rpm [54]. The decreasing trend at high disk rotation speeds is more evident for lower flow rates. On the other hand, at a constant rotation speed, the pollutant degradation increases with decreasing flow rate.

The comparison of the studies carried out in spinning disc photocatalytic reactors shows that the disc rotation speed plays a role in the degradation efficiency for three reasons. The first reason is that by increasing the disc rotation speed, centrifugal forces increase up to a certain amount (where $F \propto \omega^2 r$) and cause high shear of the liquid film on the surface of the disc and turbulence. Due to its important role in mass transfer characteristics and liquid mixing, turbulence increases with increasing rotation speed and leads to high pollutant degradation efficiency. The second reason for pollutant degradation efficiency is the thickness of the liquid film, which the Nusselt model predicts the thickness of the film on the disc surface, and there is an inverse relationship between the film thickness and the disc rotation speed (where $h \propto 1/\omega$). As the disc rotation speed increases according to equation (5), the thickness of the liquid film decreases. Decreasing the thickness of the liquid film leads to an increase in the penetration of light throughout the liquid film and the production of more radicals, thus increasing the degradation efficiency. The last reason is that unreacted pollutant molecules are quickly returned to the reaction zone. This means that increasing the rotation speed of the disc reduces the residence time and causes pollutant molecules to quickly return to the storage tank and is placed in the reactor entrance, so it returns to the reaction zone. As a result, reducing the residence time in the reaction zone reduces the degradation efficiency [49,51,75,78,83].

Another important hydrodynamic factor in SDR system is solution flow rate. The pollutant solution flow rate has different positive and negative effects on the degradation efficiency [83]. The effect of flow rate changes on the degradation of phenol pollutant in aqueous solution was investigated by Mirzaei et al. (Fig. 10) [78]. In their study, the phenol degradation efficiency increased from 81 to 87 % under constant disc rotation speed with increasing flow rate from 500 to 2500 mL/min (Fig. 10-a). Increasing the flow rate from 500 to 2500 mL/min causes strong waves on the surface of the liquid film, which leads to the creation of turbulence in the film layers, and as a result, the mass transfer coefficient and pollutant degradation increase [105]. Using the Nusselt model to determine the film thickness showed that increasing the flow rate from 500 to 2500 mL/min has increased the film thickness from 125.6 to 214.8 μm. However, according to the concentration of phenol (30 mg/l) and the molar absorption coefficient of its solution, the reduction of light penetration of the liquid film due to the increase in film thickness is insignificant [78]. Zhang et al. investigated the effect of flow rate on the degradation of phenol with a concentration of 100 mg/L (Fig. 10-b). By increasing the flow rate from 40 to 100 L/h, the

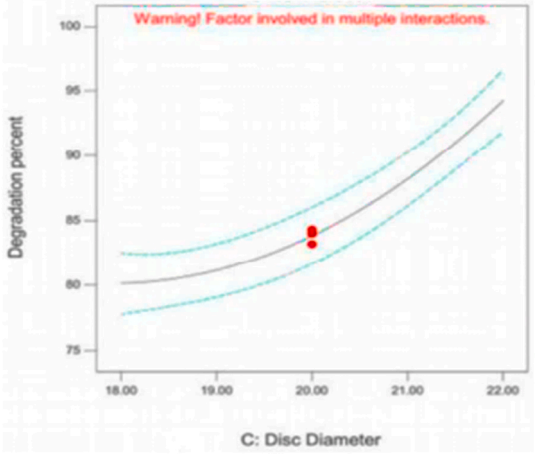

Fig. 11. Effect of disc diameter on the pollutant degradation [78].

efficiency of phenol degradation was obtained from 22.63 % to 31.85 % during a period of 120 min [76].

In general, the researchers' results showed that when the flow rate of the solution exceeds a certain value, the efficiency decreases. This behavior is probably due to the reduction of the residence time of the pollutant in the reactor, which leads to the reduction of the exposure time of the photocatalyst to light. Another reason for this could be the formation of thicker solution films, which leads to a decrease in the area of the solid-liquid interface, which reduces the degradation efficiency under these conditions. In addition to these cases, the penetration of light through the thick film is more difficult and causes the photocatalytic particles that are located deep in the film to be unable to be active. The influence of light irradiation time shows that with the increase of irradiation time due to the exposure of more photocatalytic particles to light and more activity, the degradation efficiency increases. When the flow rate is lower than a certain value, it leads to the breakdown of the film and the mixing capability of the film decreases and the degradation efficiency decreases [72]. The reason is the improper distribution of the solution on the surface of the disc and the reduction of efficiency. Therefore, by increasing the area of the interface between the photocatalyst particles and the pollutant molecules, the mass transfer rate increases and the degradation efficiency increases.

3.4.7. Effect of disc diameter

One of the factors that has not been studied much on pollutant degradation in the SDPR system is the effect of disc diameter on pollutant degradation efficiency. The only study done on this topic was done by Mirzaei et al., in 2017. They experienced discs with diameters of 18–22 cm in their research (Fig. 11). The results of their study showed that by increasing the diameter of the disc from 18 to 22 cm, the amount of phenol degradation increased from 80 to 94 %. By increasing the diameter of the disc, the surface of the catalyst exposed to light increases, and as a result, the active sites of the catalyst to produce more electron-hole pairs and more radicals are produced, which leads to an increase in the degradation efficiency [78].

3.4.8. Effect of flow regime

Various flow regimes can form on the surface of the disc depending on hydrodynamic characteristics (flow rate, disc rotational speed) and liquid physical features [44,93]. Several flow regimes (from smooth to concentric waves, irregular waves, spiral waves and film break-up) were investigated on the photocatalytic degradation of methylene blue and dehydroabetic acid on a thin film-immobilized UV-irradiated spinning disc reactor by Boiarkina et al. [44]. According to the experiments, they found that the photocatalytic surface rate for pollutant degradation is independent of flow regimes [44].

3.5. Durability test for catalytic coating on substrate surface

One of the most important features in photocatalytic degradation efficiency is the durability of coated films on the substrate. Durability and adhesion tests are performed for the strength of the bond between the substrate and the thin film of the catalyst [106]. Adhesion test shows whether the thin layer created on the substrate has the necessary resistance against distortions caused by environmental conditions such as impact caused by heavy winds, applied forces (e.g. centrifugal forces), dust impact, corrosive substances and other environmental hazards. Therefore, it is used for various adhesion test methods, such as tensile adhesion test, cross hatch, scotch tape, peeling test, scratch test, pull-off test, etc [107–110]. The only study conducted on the durability of the catalytic coating on the surface of the substrate in the spinning disc photocatalytic reactor system was conducted by Mirzaei et al., in 2017. The tensile adhesion test method was based on the applied pressure to test the durability and adhesion of the catalyst between the disc as a substrate and the thin film of the catalyst. The results of their findings under optimal conditions before and after the photocatalytic tests showed that the adhesiveness of the catalytic coating was 3.2 and 2.74 MPa, respectively. They reported that these values were due to the high thickness of the catalytic coating and the decrease in durability was due to the centrifugal force exerted by the disc rotation speed, which weakened the interface between the catalytic film and the disc surface [78]. But other studies on the durability of the catalyst on the disc surface in the SDR were carried out by conducting experiments under optimal reactor conditions during various runs. All studies showed that the efficiency of pollutant degradation remained high after several working runs, and there was no significant decrease in efficiency. Therefore, the results indicate the durability and reusability of the catalytic film [4,6,48,49,83].

3.6. Degradation mechanism in SDR

Photocatalytic mechanisms in heterojunction systems involve the interaction of different semiconductors to enhance the efficiency of photocatalysis. In a Type II heterojunction system, the photoexcited electrons and holes are spatially separated between two different semiconductors. This spatial separation reduces the recombination of charge carriers, leading to improved photocatalytic activity [111]. In a p-n heterojunction, one semiconductor is doped with p-type material (electron acceptor) and the other with n-type material (electron donor). When light is absorbed, electron-hole pairs are generated and separated at the interface between the two semiconductors, enhancing the photocatalytic process [111]. In a Z-scheme system, two different semiconductors with suitable band positions are used. The photoexcited electrons in one semiconductor are transferred to the other semiconductor, creating a continuous flow of electrons and enhancing the overall photocatalytic efficiency [112]. In an S-scheme system, two semiconductors are used where one semiconductor acts as a photosensitizer and the other as a catalyst. The photoexcited electrons from the photosensitizer are transferred to the catalyst, promoting the generation of reactive species and improving the photocatalytic activity [113,114].

Zamani et al.'s study on degradation mechanism using photocatalytic $Ag/Ag_2O/TiO_2$ p-n junction film for amoxicillin degradation in SDR system showed that when the heterojunction photocatalyst is exposed to light, photons are absorbed by the TiO_2 semiconductor, leading to the generation of electron-hole pairs. The photogenerated electrons in the TiO_2 conduction band can migrate to

the Ag metal nanoparticles due to the Schottky barrier at the Ag/TiO_2 interface. The holes in the TiO_2 valence band can migrate to the Ag_2O nanoparticles due to the favorable band alignment at the Ag_2O/TiO_2 interface. The migration of electrons and holes to the Ag and Ag_2O nanoparticles, respectively, can lead to the reduction of Ag^+ ions to Ag metal and the oxidation of Ag metal to Ag^+ ions. This redox reaction can generate reactive oxygen species (ROS) such as hydroxyl radicals and superoxide ions, which are highly reactive and can degrade organic pollutants or bacteria present in the environment [49]. In another study by Zamani andet al, the mechanism of decomposition using the $ZnO/Ag/WO_3$ S-scheme photocatalyst film for cephalexin degradation in the SDR system was shown. It was demonstrated that when Ag/WO_3 and ZnO are in close contact in a photocatalytic system, electrons flow from Ag/WO_3 to ZnO until their Fermi levels reach equilibrium, causing band bending and the formation of a potential barrier at the common interface. This process leads to the creation of an interfacial internal electric field directed from ZnO to Ag/WO_3. During light excitation, the interfacial internal electric field helps in the combination of less powerful electrons and holes on the conduction band (CB) of Ag/WO_3 and valence band (VB) of ZnO. This separation allows the stronger redox powers (the electrons on the CB of ZnO and holes on the VB of Ag/WO_3) to be geometrically separated. The more reducing electrons provide a higher driving force for the generation of O_2 radicals and the photodegradation of cephalexin. Additionally, photogenerated OH radicals attack cephalexin, leading to its complete decomposition [83]. These heterojunction systems offer unique advantages in photocatalytic processes by optimizing charge separation, enhancing redox reactions, and improving overall efficiency compared to single-component photocatalysts.

4. Conclusions

This review systematic is principally focused on pollutant degradation using the spinning disc photocatalytic reactor and effective factors on system performance. The effect of various parameters such as flow rate, disc rotation speed, flow regime, pollutant concentration, pH, reaction kinetics, radiation time, photon efficiency and radiation intensity, disc diameter, type of lamp (UV and visible) and disc surface structure are investigated. After screening the related articles that cover the purpose of the present study, it was found that in various fields, there are effective factors to achieve high performance in spinning disc photocatalytic reactors and to modify the existing challenges. In addition, various catalysts composites have been used to improve system performance and the modification of gaps created in SDR for aqueous environments treatment. Due to the effect of various parameters on the performance of spinning disc photocatalytic reactors, there are challenges in using this system on a scale-up and industrializing it, which should be resolved. Since spinning disc photocatalytic reactors have been investigated by researchers as a new system in pollutant degradation with high performance and efficiency. However, in the field of the effect of inhibitory factors, intermediate compounds resulting from degradation of pollutants, toxicity of compounds resulting from degradation, toxicity of catalysts and its leakage from the reactor, and the use of actual samples of wastewater or contaminated water has not been investigated so far. It is suggested that future research be conducted in field conditions to experiments and investigate the performance of spinning disc reactors in the degradation of different pollutants released from polluted water environments and wastewater treatment plant effluents. Also, research should be done on the stability and durability of the catalyst immobilized on the disc and the economic cost of this system compared to other photocatalytic reactors. Therefore, by optimizing the factors affecting SDR performance, scalable designs for persistent operation can be extended for industrial scale implementation. Finally, it is highly considered that the application of SRD in the photocatalytic degradation of resistant pollutants deserves further investigation and we hope that this review can be appropriate for readers who follow the aim of effective and efficient removal of pollutants and the use of this system on an industrial scale.

Data availability statement

Data will be made available on request.

Additional information

No additional information is available for this paper.

CRediT authorship contribution statement

Saeid Fallahizadeh: Writing – review & editing, Writing – original draft, Methodology, Investigation. **Mitra Gholami:** Writing – review & editing, Writing – original draft, Supervision, Methodology, Investigation. **Mahmood Reza Rahimi:** Writing – review & editing, Supervision, Methodology, Investigation. **Hamid Reza Rajabi:** Writing – review & editing, Writing – original draft, Methodology, Investigation. **Shirin Djalalinia:** Writing – review & editing, Writing – original draft, Methodology, Investigation. **Ali Esrafili:** Writing – review & editing, Writing – original draft, Methodology, Investigation. **Mahdi Farzadkia:** Writing – review & editing, Writing – original draft, Methodology, Investigation. **Majid Kermani:** Writing – review & editing, Writing – original draft, Methodology, Investigation.

Declaration of competing interest

The authors declare that they have no known competing financial interests or personal relationships that could have appeared to influence the work reported in this paper.

Acknowledgements

The authors are grateful for the financial support of the Environmental Health Technology Research Center, Iran University of Medical Sciences, Tehran, Iran (grant number: 25540 and Ethic code: IR. IUMS.REC.1402.070).

References

[1] M.P. Rayaroth, et al., Advanced oxidation processes (AOPs) based wastewater treatment-unexpected nitration side reactions-a serious environmental issue: a review, Chem. Eng. J. 430 (2022) 133002.
[2] A.O. Ibrahim, et al., Adsorptive removal of different pollutants using metal-organic framework adsorbents, J. Mol. Liq. 333 (2021) 115593.
[3] R. Chow, et al., A review of long-term pesticide monitoring studies to assess surface water quality trends, Water Res. X 9 (2020) 100064.
[4] S. Fallahizadeh, et al., Influence of integrated of activated sludge-trickling filter two-step and upflow suspended growth denitrification processes on the COD fractions in the municipal wastewaters, Int. J. Environ. Anal. Chem. 102 (8) (2022) 1735–1746.
[5] NA. Khan, et al., Hospital effluent guidelines and legislation scenario around the globe: A critical review, J. Environ. Chem. Eng. 9(5) (2021) 105874.
[6] S. Fallahizadeh, et al., Novel nanostructure approach for antibiotic decomposition in a spinning disc photocatalytic reactor, Sci. Rep. 14 (1) (2024) 10566.
[7] O.M. Rodriguez-Narvaez, et al., Treatment technologies for emerging contaminants in water: a review, Chem. Eng. J. 323 (2017) 361–380.
[8] A. Al Mayyahi, H.A.A. Al-Asadi, Advanced oxidation processes (AOPs) for wastewater treatment and reuse: a brief review, Asian J. Appl. Sci. Technol 2 (2018) 18–30.
[9] A. Srinivasan, T. Viraraghavan, Decolorization of dye wastewaters by biosorbents: a review, J. Environ. Manag. 91 (10) (2010) 1915–1929.
[10] D. Bouras, et al., Cu: ZnO deposited on porous ceramic substrates by a simple thermal method for photocatalytic application, Ceram. Int. 44 (17) (2018) 21546–21555.
[11] J. Huang, et al., Preparation of porous flower-like CuO/ZnO nanostructures and analysis of their gas-sensing property, J. Alloys Compd. 575 (2013) 115–122.
[12] G. Barzegar, et al., Ciprofloxacin degradation by catalytic activation of monopersulfate using Mn–Fe oxides: performance and mineralization, Water Sci. Technol. 87 (5) (2023) 1029–1042.
[13] Z.H. Jabbar, et al., Rational design of novel 0D/0D Bi2Sn2O7/CeO2 in the core-shell nanostructure for boosting the photocatalytic decomposition of antibiotics in wastewater: S-type-based mechanism, Mater. Sci. Semicond. Process. 173 (2024) 108165.
[14] Z. Xu, et al., Fabrication of 2D/2D Z-scheme highly crystalline carbon nitride/δ-Bi2O3 heterojunction photocatalyst with enhanced photocatalytic degradation of tetracycline, J. Alloys Compd. 895 (2022) 162667.
[15] S. Fallahizadeh, et al., Enhanced photocatalytic degradation of amoxicillin using a spinning disc photocatalytic reactor (SDPR) with a novel Fe3O4@ void@ CuO/ZnO yolk-shell thin film nanostructure, Sci. Rep. 13 (1) (2023) 16185.
[16] D.I. Anwar, D. Mulyadi, Synthesis of Fe-TiO2 composite as a photocatalyst for degradation of methylene blue, Procedia Chem. 17 (2015) 49–54.
[17] M. Uddin, et al., Influence of TiO2 and ZnO photocatalysts on adsorption and degradation behaviour of Erythrosine, Dyes Pigments 75 (1) (2007) 207–212.
[18] S.M.d.A.G. Ulson, K.A.S. Bonilla, A.A.U. de Souza, Removal of COD and color from hydrolyzed textile azo dye by combined ozonation and biological treatment, J. Hazard Mater. 179 (1–3) (2010) 35–42.
[19] P. Bhattacharya, et al., Combination technology of ceramic microfiltration and reverse osmosis for tannery wastewater recovery, Water Resour. Ind. 3 (2013) 48–62.
[20] M. Elias, et al., Fabrication of Zn3 (PO4) 2/carbon nanotubes nanocomposite thin film via sol-gel drop coating method with enhanced photocatalytic activity, Thin Solid Films 717 (2021) 138472.
[21] M. Muruganandham, I. Chen, J. Wu, Effect of temperature on the formation of macroporous ZnO bundles and its application in photocatalysis, J. Hazard Mater. 172 (2–3) (2009) 700–706.
[22] I.M. Cardoso, R.M. Cardoso, J.C.E. da Silva, Advanced oxidation processes coupled with nanomaterials for water treatment, Nanomaterials 11 (8) (2021) 2045.
[23] M. Kurian, Advanced oxidation processes and nanomaterials-a review, Cleaner Engineering and Technology 2 (2021) 100090.
[24] M.H. Mahdi, T.J. Mohammed, J.A. Al-Najar, Advanced Oxidation Processes (AOPs) for treatment of antibiotics in wastewater: a review, in: IOP Conference Series: Earth and Environmental Science, IOP Publishing, 2021.
[25] A. Majumdar, A. Pal, Recent advancements in visible-light-assisted photocatalytic removal of aqueous pharmaceutical pollutants, Clean Technol. Environ. Policy 22 (1) (2020) 11–42.
[26] K. Ikehata, N. Jodeiri Naghashkar, M. Gamal El-Din, Degradation of aqueous pharmaceuticals by ozonation and advanced oxidation processes: a review, Ozone Sci. Eng. 28 (6) (2006) 353–414.
[27] O. Máynez-Navarro, J. Sanchez-Salas, Focus on zinc oxide as a photocatalytic material for water treatment, Int. J. Bioremediation Biodegrad 1 (2018).
[28] V.O. Shikuku, W.N. Nyairo, Advanced oxidation processes for dye removal from wastewater, in: Impact of Textile Dyes on Public Health and the Environment, IGI Global, 2020, pp. 205–238.
[29] K.P. Sundar, S. Kanmani, Progression of Photocatalytic reactors and it's comparison: a Review, Chem. Eng. Res. Des. 154 (2020) 135–150.
[30] R. Molinari, et al., Photocatalytic Processes in Membrane Reactors, Comprehensive Membrane Science and Engineering (2017) 101–138.
[31] Y. Chen, E. Stathatos, D.D. Dionysiou, Microstructure characterization and photocatalytic activity of mesoporous TiO2 films with ultrafine anatase nanocrystallites, Surf. Coating. Technol. 202 (10) (2008) 1944–1950.
[32] G. Camera-Roda, et al., Guidelines for the assessment of the rate law of slurry photocatalytic reactions, Catal. Today 281 (2017) 221–230.
[33] R.L. Pozzo, M.A. Baltanas, A.E. Cassano, Supported titanium oxide as photocatalyst in water decontamination: state of the art, Catal. Today 39 (3) (1997) 219–231.
[34] Y. Yang, P. Wang, Preparation and characterizations of a new PS/TiO2 hybrid membranes by sol–gel process, Polymer 47 (8) (2006) 2683–2688.
[35] H. Li, Z. Mu, Q. Sha, Ag/AgCl coupled with WO3 films on glass slides and enhanced photocatalysis performance under visible light, Mater. Res. Express 6 (9) (2019) 096421.
[36] A. Baglov, et al., Photocatalytic activity of nanostructured titania coatings on aluminum substrates, Inorg. Mater. 53 (11) (2017) 1180–1184.
[37] M. Hatat-Fraile, et al., Concurrent photocatalytic and filtration processes using doped TiO2 coated quartz fiber membranes in a photocatalytic membrane reactor, Chem. Eng. J. 330 (2017) 531–540.
[38] K. Sirirerkratana, P. Kemacheevakul, S. Chuangchote, Color removal from wastewater by photocatalytic process using titanium dioxide-coated glass, ceramic tile, and stainless steel sheets, J. Clean. Prod. 215 (2019) 123–130.
[39] D. Marković, et al., Sonophotocatalytic degradation of dye CI Acid Orange 7 by TiO2 and Ag nanoparticles immobilized on corona pretreated polypropylene non-woven fabric, Ultrason. Sonochem. 24 (2015) 221–229.
[40] D. Prieling, H. Steiner, Analysis of the wall mass transfer on spinning disks using an integral boundary layer method, Chem. Eng. Sci. 101 (2013) 109–119.
[41] W.H. Khan, V.K. Rathod, Process intensification approach for preparation of curcumin nanoparticles via solvent–nonsolvent nanoprecipitation using spinning disc reactor, Chem. Eng. Process: Process Intensif. 80 (2014) 1–10.
[42] A. Aoune, C. Ramshaw, Process intensification: heat and mass transfer characteristics of liquid films on rotating discs, Int. J. Heat Mass Tran. 42 (14) (1999) 2543–2556.
[43] K. Boodhoo, R. Jachuck, Process intensification: spinning disk reactor for styrene polymerisation, Appl. Therm. Eng. 20 (12) (2000) 1127–1146.
[44] I. Boiarkina, S. Pedron, D.A. Patterson, An experimental and modelling investigation of the effect of the flow regime on the photocatalytic degradation of methylene blue on a thin film coated ultraviolet irradiated spinning disc reactor, Appl. Catal. B Environ. 110 (2011) 14–24.
[45] K.-J. Chen, Y.-S. Chen, Intensified production of biodiesel using a spinning disk reactor, Chem. Eng. Process: Process Intensif. 78 (2014) 67–72.

[46] X. Feng, et al., The spinning cloth disc reactor for immobilized enzymes: a new process intensification technology for enzymatic reactions, Chem. Eng. J. 221 (2013) 407–417.
[47] H.-S. Liu, et al., Characterization of AgI nanoparticles synthesized in a spinning disk reactor, Chem. Eng. J. 183 (2012) 466–472.
[48] A. Expósito, et al., Antipyrine removal by TiO2 photocatalysis based on spinning disc reactor technology, J. Environ. Manag. 187 (2017) 504–512.
[49] S. Zamani, M. Rahimi, M. Ghaedi, Spinning disc photoreactor based visible-light-driven Ag/Ag2O/TiO2 heterojunction photocatalyst film toward the degradation of amoxicillin, J. Environ. Manag. 303 (2022) 114216.
[50] S. Zamani, M.R. Rahimi, M. Ghaedi, Photocatalytic degradation of penicillin v using Bi2O3/Ag/TiO2 thin film in a spinning disc photoreactor under blue LED illumination, Iran, J. Chem. Chem. Eng. (Int. Engl. Ed.) 41 (9) (2022) 3032–3044.
[51] I. Boiarkina, S. Norris, D.A. Patterson, The case for the photocatalytic spinning disc reactor as a process intensification technology: comparison to an annular reactor for the degradation of methylene blue, Chem. Eng. J. 225 (2013) 752–765.
[52] D.D. Dionysiou, et al., Rotating disk photocatalytic reactor: development, characterization, and evaluation for the destruction of organic pollutants in water, Water Res. 34 (11) (2000) 2927–2940.
[53] Y. Chen, D.D. Dionysiou, TiO2 photocatalytic films on stainless steel: the role of Degussa P-25 in modified sol–gel methods, Appl. Catal. B Environ. 62 (3–4) (2006) 255–264.
[54] C.-Y. Chang, N.-L. Wu, Process analysis on photocatalyzed dye decomposition for water treatment with TiO2-coated rotating disk reactor, Ind. Eng. Chem. Res. 49 (23) (2010) 12173–12179.
[55] T. McMurray, et al., Intrinsic kinetics of photocatalytic oxidation of formic and oxalic acid on immobilised TiO2 films, Appl. Catal. Gen. 262 (1) (2004) 105–110.
[56] Z. Cheng, et al., Photocatalytic degradation of bisphenol A using an integrated system of a new gas-liquid-solid circulating fluidized bed reactor and micrometer Gd-doped TiO2 particles, J. Environ. Sci. 24 (7) (2012) 1317–1326.
[57] M.-J. Kim, K.-H. Choo, H.-S. Park, Photocatalytic degradation of seawater organic matter using a submerged membrane reactor, J. Photochem. Photobiol. Chem. 216 (2–3) (2010) 215–220.
[58] C. McCullagh, et al., Photocatalytic reactors for environmental remediation: a review, J. Chem. Technol. Biotechnol. 86 (8) (2011) 1002–1017.
[59] C. McCullagh, et al., Development of a slurry continuous flow reactor for photocatalytic treatment of industrial waste water, J. Photochem. Photobiol. Chem. 211 (1) (2010) 42–46.
[60] B. Srikanth, et al., Recent advancements in supporting materials for immobilised photocatalytic applications in waste water treatment, J. Environ. Manag. 200 (2017) 60–78.
[61] H.I. De Lasa, B. Serrano, M. Salaices, Photocatalytic Reaction Engineering, Springer, 2005.
[62] G. Mascolo, et al., Photocatalytic degradation of methyl red by TiO2: comparison of the efficiency of immobilized nanoparticles versus conventional suspended catalyst, J. Hazard Mater. 142 (1–2) (2007) 130–137.
[63] G. Vilardi, et al., Production of nano Zero Valent Iron particles by means of a spinning disk reactor, Chemical engineering transactions 57 (2017) 751–756.
[64] K. Boodhoo, A. Harvey, Process Intensification Technologies for Green Chemistry: Engineering Solutions for Sustainable Chemical Processing, John Wiley & Sons, 2013.
[65] A. Zhang, et al., The combination of rotating disk photocatalytic reactor and TiO2 nanotube arrays for environmental pollutants removal, J. Hazard Mater. 186 (2–3) (2011) 1374–1383.
[66] G. Sharma, et al., Nanophotocatalysis and Environmental Applications: Materials and Technology, vol. 29, Springer, 2019.
[67] D. Wang, et al., Regulation of velocity zoning behaviour and hydraulic jump of impinging jet flow on a spinning disk reactor, Chem. Eng. J. 390 (2020) 124392.
[68] H. Abdullah, A. Al-Amiery, S. Al-Baghdadi, The using of nanomaterials as catalysts for photodegradations, in: Journal of Physics: Conference Series, IOP Publishing, 2021.
[69] J. Burns, C. Ramshaw, R. Jachuck, Measurement of liquid film thickness and the determination of spin-up radius on a rotating disc using an electrical resistance technique, Chem. Eng. Sci. 58 (11) (2003) 2245–2253.
[70] I. Tsibranska, et al., Modelling of mass transfer in film flow of shear thinning liquid on a horizontal rotating disk, Chem. Eng. Process: Process Intensif. 48 (3) (2009) 823–827.
[71] L.-B. Yao, et al., Intensification of micromixing efficiency in a spinning disk reactor: experimental investigation, Chemical Engineering and Processing-Process Intensification 166 (2021) 108500.
[72] K.V. Boodhoo, S.R. Al-Hengari, Micromixing characteristics in a small-scale spinning disk reactor, Chem. Eng. Technol. 35 (7) (2012) 1229–1237.
[73] A.N.M. Martínez, et al., Effects of increased viscosity on micromixing in rotor-stator spinning disk reactors, Chem. Eng. J. (2022) 134292.
[74] D. Moher, et al., Preferred reporting items for systematic reviews and meta-analyses: the PRISMA statement, Ann. Intern. Med. 151 (4) (2009) 264–269.
[75] I. Boiarkina, S. Norris, D.A. Patterson, Investigation into the effect of flow structure on the photocatalytic degradation of methylene blue and dehydroabietic acid in a spinning disc reactor, Chem. Eng. J. 222 (2013) 159–171.
[76] Q. Zhang, et al., Investigation of enhancement of spinning disk reactor on the degradation of phenol wastewater by photocatalytic system, J. Chem. Eng. Jpn. 52 (6) (2019) 528–535.
[77] C.-N. Lin, et al., Photocatalytic degradation of methyl orange by a multi-layer rotating disk reactor, Environ. Sci. Pollut. Control Ser. 19 (9) (2012) 3743–3750.
[78] M. Mirzaei, et al., Photocatalysis of phenol using a spinning disc photoreactor immobilized with TiO2 nanoparticles: hydrodynamic modeling and reactor optimization, Ind. Eng. Chem. Res. 56 (7) (2017) 1739–1749.
[79] M. Mirzaei, et al., Evaluation and modeling of a spinning disc photoreactor for degradation of phenol: impact of geometry modification, J. Photochem. Photobiol. Chem. 346 (2017) 206–214.
[80] H. Yatmaz, C. Wallis, C. Howarth, The spinning disc reactor–studies on a novel TiO2 photocatalytic reactor, Chemosphere 42 (4) (2001) 397–403.
[81] M.A. Behnajady, H. Dadkhah, H. Eskandarloo, Horizontally rotating disc recirculated photoreactor with TiO2-P25 nanoparticles immobilized onto a HDPE plate for photocatalytic removal of p-nitrophenol, Environ. Technol. 39 (8) (2018) 1061–1070.
[82] H.J. Huang, B.-H. Liu, J.A. Yeh, Ammonium oxidization at room temperature and plasmonic photocatalytic enhancement, Catal. Commun. 36 (2013) 16–19.
[83] S. Zamani, et al., WO3/Ag/ZnO S-scheme heterostructure thin film spinning disc photoreactor for intensified photodegradation of cephalexin antibiotic, Chemosphere 307 (2022) 135812.
[84] H.J. Huang, K.-C. Huang, D.P. Tsai, Light absorption measurement of a plasmonic photocatalyst in the circular plane waveguide of a photocatalytic dual light source spinning disk reactor, Opt. Rev. 20 (2) (2013) 236–240.
[85] A. Mills, C. O'Rourke, K. Moore, Powder semiconductor photocatalysis in aqueous solution: an overview of kinetics-based reaction mechanisms, J. Photochem. Photobiol. Chem. 310 (2015) 66–105.
[86] J.Z. Bloh, A holistic approach to model the kinetics of photocatalytic reactions, Front. Chem. 7 (2019) 128.
[87] I. Grcić, G. Li Puma, Photocatalytic degradation of water contaminants in multiple photoreactors and evaluation of reaction kinetic constants independent of photon absorption, irradiance, reactor geometry, and hydrodynamics, Environ. Sci. Technol. 47 (23) (2013) 13702–13711.
[88] S. Mozia, et al., Application of anatase-phase TiO2 for decomposition of azo dye in a photocatalytic membrane reactor, Desalination 241 (1–3) (2009) 97–105.
[89] I. Poulios, I. Aetopoulou, Photocatalytic degradation of the textile dye reactive orange 16 in the presence of TiO2 suspensions, Environ. Technol. 20 (5) (1999) 479–487.
[90] R. Binjhade, R. Mondal, S. Mondal, Continuous photocatalytic reactor: critical review on the design and performance, J. Environ. Chem. Eng. (2022) 107746.
[91] A.M. Ali, E.A. Emanuelsson, D.A. Patterson, Photocatalysis with nanostructured zinc oxide thin films: the relationship between morphology and photocatalytic activity under oxygen limited and oxygen rich conditions and evidence for a Mars Van Krevelen mechanism, Appl. Catal. B Environ. 97 (1–2) (2010) 168–181.

[92] A.M. Ali, E.A. Emanuelsson, D.A. Patterson, Conventional versus lattice photocatalysed reactions: implications of the lattice oxygen participation in the liquid phase photocatalytic oxidation with nanostructured ZnO thin films on reaction products and mechanism at both 254 nm and 340 nm, Appl. Catal. B Environ. 106 (3–4) (2011) 323–336.
[93] A. Charwat, R. Kelly, C. Gazley, The flow and stability of thin liquid films on a rotating disk, J. Fluid Mech. 53 (2) (1972) 227–255.
[94] T. Van Gerven, et al., A review of intensification of photocatalytic processes, Chem. Eng. Process: Process Intensif. 46 (9) (2007) 781–789.
[95] C.C.d. Escobar, J.H.Z.d. Santos, Nanostructured imprinted supported photocatalysts: organic and inorganic matrixes, in: Nanophotocatalysis and Environmental Applications, Springer, 2019, pp. 1–48.
[96] R. Gorges, S. Meyer, G. Kreisel, Photocatalysis in microreactors, J. Photochem. Photobiol. Chem. 167 (2–3) (2004) 95–99.
[97] P. Bansal, A. Verma, In-situ dual effect studies using novel Fe-TiO2 composite for the pilot-plant degradation of pentoxifylline, Chem. Eng. J. 332 (2018) 682–694.
[98] J. Shen, J. Tower, Effects of light on aging and longevity, Ageing Res. Rev. 53 (2019) 100913.
[99] E. Austin, et al., Visible light. Part I: properties and cutaneous effects of visible light, J. Am. Acad. Dermatol. 84 (5) (2021) 1219–1231.
[100] M. Chahkandi, M. Zargazi, New water based EPD thin BiVO4 film: effective photocatalytic degradation of Amoxicillin antibiotic, J. Hazard Mater. 389 (2020) 121850.
[101] O. Carp, C.L. Huisman, A. Reller, Photoinduced reactivity of titanium dioxide, Prog. Solid State Chem. 32 (1–2) (2004) 33–177.
[102] D. Ghiasy, K. Boodhoo, M. Tham, Control of intensified equipment: a simulation study for pH control in a spinning disc reactor, Chem. Eng. Process: Process Intensif. 55 (2012) 1–7.
[103] D.D. Dionysiou, et al., Oxidation of organic contaminants in a rotating disk photocatalytic reactor: reaction kinetics in the liquid phase and the role of mass transfer based on the dimensionless Damköhler number, Appl. Catal. B Environ. 38 (1) (2002) 1–16.
[104] S.M. Meunier, et al., Design and characterization of a novel rotating corrugated drum reactor for wastewater treatment, Int. J. Photoenergy (2010) 2010.
[105] S. Mohammadi, K.V. Boodhoo, Online conductivity measurement of residence time distribution of thin film flow in the spinning disc reactor, Chem. Eng. J. 207 (2012) 885–894.
[106] V. Lukong, et al., Annealing temperature variation and its influence on the self-cleaning properties of TiO2 thin films, Heliyon (2022) e09460.
[107] P. Benjamin, C. Weaver, Measurement of adhesion of thin films, Proc. Roy. Soc. Lond. Math. Phys. Sci. 254 (1277) (1960) 163–176.
[108] M. Wu, et al., Highly transparent low resistance ATO/AgNWs/ATO flexible transparent conductive thin films, Ceram. Int. 46 (4) (2020) 4344–4350.
[109] K.P. Marimuthu, et al., Influence of substrate type and film thickness on the failures of Zr-based thin-film metallic glass under nanoscratch, Wear 494 (2022) 204241.
[110] S. Manna, M.K. Naskar, S.K. Medda, Mesoporous silica-based abrasion resistant antireflective (AR)-cum-hydrophobic coatings on textured solar cover glasses by a spray coating technique, Materials Advances 3 (7) (2022) 3208–3217.
[111] Z.H. Jabbar, et al., The latest progress in the design and application of semiconductor photocatalysis systems for degradation of environmental pollutants in wastewater: mechanism insight and theoretical calculations, Mater. Sci. Semicond. Process. 173 (2024) 108153.
[112] M. Amiri, et al., Bi 2 WO 6/Ag 3 PO 4–Ag Z-scheme heterojunction as a new plasmonic visible-light-driven photocatalyst: performance evaluation and mechanism study, New J. Chem. 43 (3) (2019) 1275–1284.
[113] Z.H. Jabbar, et al., A critical review describes wastewater photocatalytic detoxification over Bi5O7I-based heterojunction photocatalysts: characterizations, mechanism insight, and DFT calculations, J. Environ. Chem. Eng. (2024) 112241.
[114] Z.H. Jabbar, et al., Reasonable decoration of CuO/Cd0. 5Zn0. 5S nanoparticles onto flower-like Bi5O7I as boosted step-scheme photocatalyst for reinforced photodecomposition of bisphenol A and Cr (VI) reduction in wastewater, J. Environ. Manag. 348 (2023) 119302.